THE ABSOLUTE CROSS SECTION FOR THE REACTION $D(p,\gamma)^3He$ FROM 400 KeV TO 1100 KeV

by

RICHARD LLOYD HELMER

B.A.Sc., University of British Columbia, 1966

A THESIS SUBMITTED IN PARTIAL FULFILLMENT OF

THE REQUIREMENTS FOR THE DEGREE OF

MASTER OF APPLIED SCIENCE

in the Department

of

PHYSICS

We accept this thesis as conforming to the

required standard

THE UNIVERSITY OF BRITISH COLUMBIA

April, 1969

In presenting this thesis in partial fulfilment of the requirements for an advanced degree at the University of British Columbia, I agree that the Library shall make it freely available for reference and study. I further agree that permission for extensive copying of this thesis for scholarly purposes may be granted by the Head of my Department or by his representatives. It is understood that copying or publication of this thesis for financial gain shall not be allowed without my written permission.

Department of Physics

The University of British Columbia
Vancouver 8, Canada

Date: April, 1969

ABSTRACT

The absolute cross section of the reaction $D(p,\gamma)^3He$ has been measured in the energy range from 400 Kev to 1100 Kev in the laboratory system. A target of deuterated polyethylene was used to measure the relative yield of the reaction over this range, and the results were normalized to an absolute measurement made with a deuterium gas target.

The reaction is of interest because it enables some information to be obtained about the forces binding three nucleons together. It also has some significance in a number of astrophysical processes.

In order to determine the cross section, the intrinsic efficiency of a 5 inch by 4 inch sodium iodide crystal scintillation counter was measured by simultaneous alpha particle and gamma ray counting on the 340 Kev resonance of the reaction $^{19}F(p,\alpha\gamma)^{16}O$. The intrinsic efficiency of the detector was found to be $.679 \pm .03$ for the 6.14 Mev gamma rays from this reaction, with the particular geometry used.

The absolute cross section for the reaction $D(p,\gamma)^3He$ was found by the gas target measurement to be $2.33 \pm .07$ microbarns for an incident proton energy of 643 kev.

TABLE OF CONTENTS

LIST OF TABLES

LIST OF FIGURES

ACKNOWLEDGEMENTS

I wish to express my gratitude to all the members of the Van de Graaff group for their help during the course of this work. Particular thanks go to Dr. G. M. Bailey for his supervision of the experimental part, and to Dr. G. M. Griffiths for his assistance and very helpful suggestions during the writing of this thesis.

CHAPTER I

INTRODUCTION

1.1 General Introduction

One key to understanding the properties of nuclei would be to discover the characteristics of the internucleon force. A correlation exists between various parts of the nuclear force and the detailed character of nuclear bound state wave functions. Since many theoretical studies have been made to relate details of the force system in a quantitative way to the properties of few nucleon systems, it is important to obtain as much experimental information as possible about the bound states of nuclei, and particularly light nuclei, where the many body aspects of the problem do not obscure the specific relations between nuclear structure and characteristics of the internucleon force.

Direct radiative capture reactions provide a relatively simple way of determining some of the properties of nuclear bound states and assessing nuclear models through comparing theoretically predicted and experimentally measured cross sections. The simplicity in comparison to other reactions arises because the transition which proceeds directly from a free nucleon state to a bound state is produced by a relatively weak coupling to the electromagnetic radiation field which does not produce a large perturbation on the system. Other direct reactions might be used to study the bound states, for example, the stripping reaction, in which one nucleon from an incoming complex particle is stripped off the complex and moves directly to a final bound state without forming an intermediate compound state. In this case the interaction between particles occurs through the medium of another particle and involves strong

nuclear forces. This makes it much more difficult to extract information about the nuclear forces since a knowledge of the nuclear forces is required to understand the nature of the transition from one nuclear state to another.

For the above reason and for further reasons noted below, a study of the direct radiative capture of protons by deuterium to form ^{3}He should prove useful in understanding the 3 nucleon system. First, this reaction results in the formation of ^{3}He, which is more tightly bound than the deuteron, the only bound two body nucleus. Also ^{3}He has both singlet and triplet two-nucleon spin configurations while the deuteron has only the triplet configuration. Thus the structure of ^{3}He should be more sensitive to the short range components of the nuclear force as well as to the components which depend on the singlet spin configuration. Therefore a study of three body nuclei should provide more information about the internucleon force than can be obtained from the deuteron.

Another reason why this reaction is of interest is related to astrophysics. The reaction $D(p,\gamma)^3He$ is the second step in the chain of reactions which supplies most of the energy in the hydrogen-burning stage of the smaller main-sequence stars. This chain is as follows:

$$p + p \rightarrow D + \beta^+ + \nu$$

$$p + D \rightarrow {}^3He + \gamma$$

$${}^3He + {}^3He \rightarrow {}^4He + 2p$$

Now although the rate of energy release of a main sequence star is controlled by the first reaction since it occurs by means of the very weak β-interaction, it is likely that the reaction $D(p,\gamma)^3He$ is the first to supply nuclear energy as the star contracts, and it may consequently have considerable effect on the rate at which the star condenses to the main sequence, at least if there is as high a deuterium to hydrogen ratio in the interstellar gas as is found in the earth.

In the early stages of stellar condensation, the reaction $D(p,\gamma)^3He$

competes with the reaction $D(d,n)^3He$ which has a much larger cross section, but a smaller probability of occurring since the concentration of hydrogen is much greater than the concentration of deuterium. The latter reaction supplies neutrons to the interstellar gas which are then captured by the heavy elements and thus there may be significant changes in some isotope ratios from the primordial ratios depending on the number of neutrons supplied. Clearly the number of neutrons available for this process is dependent upon the initial concentration of deuterium and the amount of it that survives long enough to produce neutrons. Thus the isotope ratios among the heavy elements could be affected by the reaction $D(p,\gamma)^3He$, since much of the deuterium which would otherwise be available for the release of neutrons is removed by this reaction.

1.2 Previous Work

Previous work on the reaction by Fowler, Lauritsen and Tollestrup (FO 49) indicated that the angular distribution was of the form $a + b \sin^2\theta$ where the isotropic part a was small but not zero. The presence of the $\sin^2\theta$ component in the angular distribution led these workers to advance the hypothesis that the capture was mainly the result of an electric dipole transition of a p-wave proton to the ground S - state of ^3He. Their investigation of the yield at 90^0 for various bombarding energies showed that the reaction was non-resonant in character, indicative of a direct capture process.

In an ingenious experiment, Wilkinson (WI 52) showed that the gamma radiation at 90^0 was plane polarized with the electric dipole in the reaction plane. This confirmed the hypothesis of Fowler et. al. that the capture was the result of an E1 transition. Wilkinson also suggested that the small isotropic component could arise from a small amount of spin-orbit coupling. However, Griffiths and Warren (GR 55) found that the energy dependence of the yield was different at 90^0 from what it was at 0^0, and this raised the possibility that the isotropic component might arise from S-wave capture of the

incoming protons. Verde (VE 50) had shown that magnetic dipole transitions could occur between S-states of the continuum and the bound three nucleon S-state as a result of small non-central components in the nuclear force. Further measurement by Griffiths et. al. (GR 63) in the energy range from 25 Kev to 45 Kev confirmed the hypothesis that the yield at 0^{o} followed an energy dependence characteristic of incoming S-waves.

The ground state of ^{3}He is known to have $J^{\pi} = \frac{1}{2}^{+}$, and thus can contain the components (SA 55):

$$^{2}S_{\frac{1}{2}} \qquad ^{2,4}P_{\frac{1}{2}} \qquad ^{4}D_{\frac{1}{2}}$$

However, Derrick (De 60) has shown that the amplitudes of the ^{2}P and ^{4}P components are negligible. The continuum states arising from the unbound p + D system contains the following components which can give rise to electromagnetic transitions to the bound state components:

$$^{4}S \qquad ^{2,4}P \qquad ^{2}D \qquad ^{4}P$$

Thus the E1 radiation is the result of transitions from ^{2}P to $^{2}S_{\frac{1}{2}}$ states which gives rise to the main $\sin^{2}\theta$ part of the angular distribution. The isotropic part arises mainly from M1 radiation, which results from transitions from ^{4}S to $^{2}S_{\frac{1}{2}}$ states. Other transitions which could be of some significance are the following: E2 ($^{2}D - {}^{2}S$), E1($^{4}P - {}^{4}D$), E1($^{4}F - {}^{4}D$) and E2($^{4}S - {}^{4}D$). There are also some interference terms. The most important of these is the E1($^{2}P - {}^{2}S$)/E2($^{2}D - {}^{2}S$) interference.

Donnelly (DO 68) has investigated the effects of these transitions and their interferences theoretically. His results are based mainly on a two body model describing the interaction between a proton and deuteron but incorporating some three body parameters in an empirical way. It is important that his findings be checked experimentally to determine whether this is a useful

model for the reaction, and if so, to try to extract some theoretically significant parameters from the data. It is of particular importance to investigate the cross sections predicted by this semi-empirical theory, since if these do not compare favorably with experiment, it is unlikely that any of the other parameters will be particularly significant. Other work has been done recently in this laboratory to measure the angular distribution of the emitted radiation, however the main object of the present work was to measure the absolute cross section of the reaction as accurately as possible.

CHAPTER II

THEORY

A brief description of the parameters required for the determination of the cross section is given in this chapter.

2.1 The Angular Distribution

The measured angular distribution of the reaction $D(p,\gamma)^3He$ can be described as a series of Legendre polynomials in the form

$$W(\theta') = \sum_{\ell=0}^{r} B_\ell P_\ell (\cos\theta') \qquad (2.1 - 1)$$

where θ' is measured in the center of mass system.

Before the experimental angular distribution can be compared with the theory, it must be corrected for the finite solid angle of the detector. It has been shown by Rose (RO 53) that for an angular distribution of the form (2.1 - 1), these corrections are particularly simple. The corrected angular distribution is given by

$$W(\theta') = \sum_{\ell=0}^{r} A_\ell P_\ell (\cos\theta) \qquad (2.1 - 2)$$

where $A_\ell = B_\ell / Q_\ell$.

The so-called smoothing factors, Q_ℓ take into account the smearing of the angular distribution which results from the finite solid angle of the detector. They are given by J_ℓ / J_o , where J_ℓ is obtained from the following integral.

$$J_\ell = \int_0^\beta P_\ell(\cos\zeta)\left[1 - e^{-\mu x(\zeta)}\right] \sin\zeta \, d\zeta \qquad (2.1 - 3)$$

where β is the half angle of the detector

μ is the linear attenuation coefficient

$x(\zeta)$ is the distance traversed by radiation incident on the crystal at an angle ζ to the axis

and P_ℓ are the Legendre polynomials of order ℓ.

Now the angular distribution given by (2.1 - 2) is essentially the differential cross section $\frac{\partial \sigma}{\partial \Omega}$, and from this one can determine the expected gamma ray yield, $N_\gamma(\theta)$, at a particular angle θ, by integrating over the solid angle subtended by the detector at the source. The expression obtained from this integration is

$$N_\gamma(\theta) = N_p N_D \varepsilon \Omega_{Det.} A_o \left[1 + \frac{A_1}{A_o} P_1 Q_1 + \frac{A_2}{A_o} P_2 Q_2 + \frac{A_3}{A_o} P_3 Q_3\right] \qquad (2.1 - 4)$$

where N_p = number of incident protons

N_D = number of target atoms per square centimeter

ε = efficiency of the detector

$\Omega_{Det.}$ = solid angle subtended by the detector at the source.

Terms for angular momentum ℓ greater than three have not been included since it has been shown (DO 67) that the cross section for the $\ell = 4$ term, which would arise from an E2 ($^2D - {}^2S$) transition is very small compared to the main E1 ($^2p - {}^2S$) transition.

The form of the angular distribution given in Chapter I implies that the maximum yield is obtained at a laboratory angle of 90° to the incident proton beam, and hence from the point of view of the statistical significance of the number of counts obtained, it is best to measure the gamma ray yield at this angle.

Now the total cross section is obtained from an integration over all angles of (2.1 - 2), and the result is

$$\sigma_T = 4\pi A_o \qquad (2.1 - 5)$$

where A_o is given by (2.1 - 4).

Thus the total cross section for a given energy E, $\sigma_T(\epsilon)$ is computed by combining the last two equations to obtain

$$\sigma_T(E) = \frac{4\pi\, N_\gamma(E)_{\theta=90^\circ}}{N_P N_D \varepsilon \Omega_{Det} \left[1 + \frac{A_1}{A_o} P_1 Q_1 + \frac{A_2}{A_o} P_2 Q_2 + \frac{A_3}{A_o} P_3 Q_3\right]} \qquad (2.1 - 6)$$

where $N_\gamma(E)_{\theta=90^\circ}$ is the gamma ray yield obtained at $\theta = 90^\circ$ for a given energy E and the Legendre polynomials P_1, P_2 and P_3 are evaluated for $\theta = 90^\circ$.

The other parameters are as previously described.

The expression (2.1 - 6) shows that before the total cross section can be determined it is necessary to measure the angular distribution in order to obtain the ratio of the coefficients $\left(\frac{A_1}{A_o}\right)$, $\left(\frac{A_2}{A_o}\right)$ and $\left(\frac{A_3}{A_o}\right)$ for a given energy E at which the cross section is to be measured. The measurements of the angular distribution has been made at laboratory proton energies of 500 Kev 650 Kev and 800 Kev (BA 69). From a least squares fit of these angular distribution measurements, the ratios of the coefficients were determined. The results are listed in Table II - 1. and are shown in Figure II - 1. The other results shown in this figure are from data obtained by previous workers.

Table II - 1 : Ratios of Coefficients from the Angular Distribution Measurements.

Ep (lab)	$A_1/A_o = -A_3/A_o$	A_2/A_o
455 kev	.072 $\pm$ .012	-.940 $\pm$ .012
595 kev	.115 $\pm$ .013	-.965 $\pm$ .013
760 kev	.127 $\pm$ .016	-.958 $\pm$ .013

The values of the smoothing factors for the detector geometry used in this experiment are listed in Table II - 2. These were obtained from the computer program DEWF, which was written previously (LE 64) to evaluate numerically the integral given in (2.1 - 3)

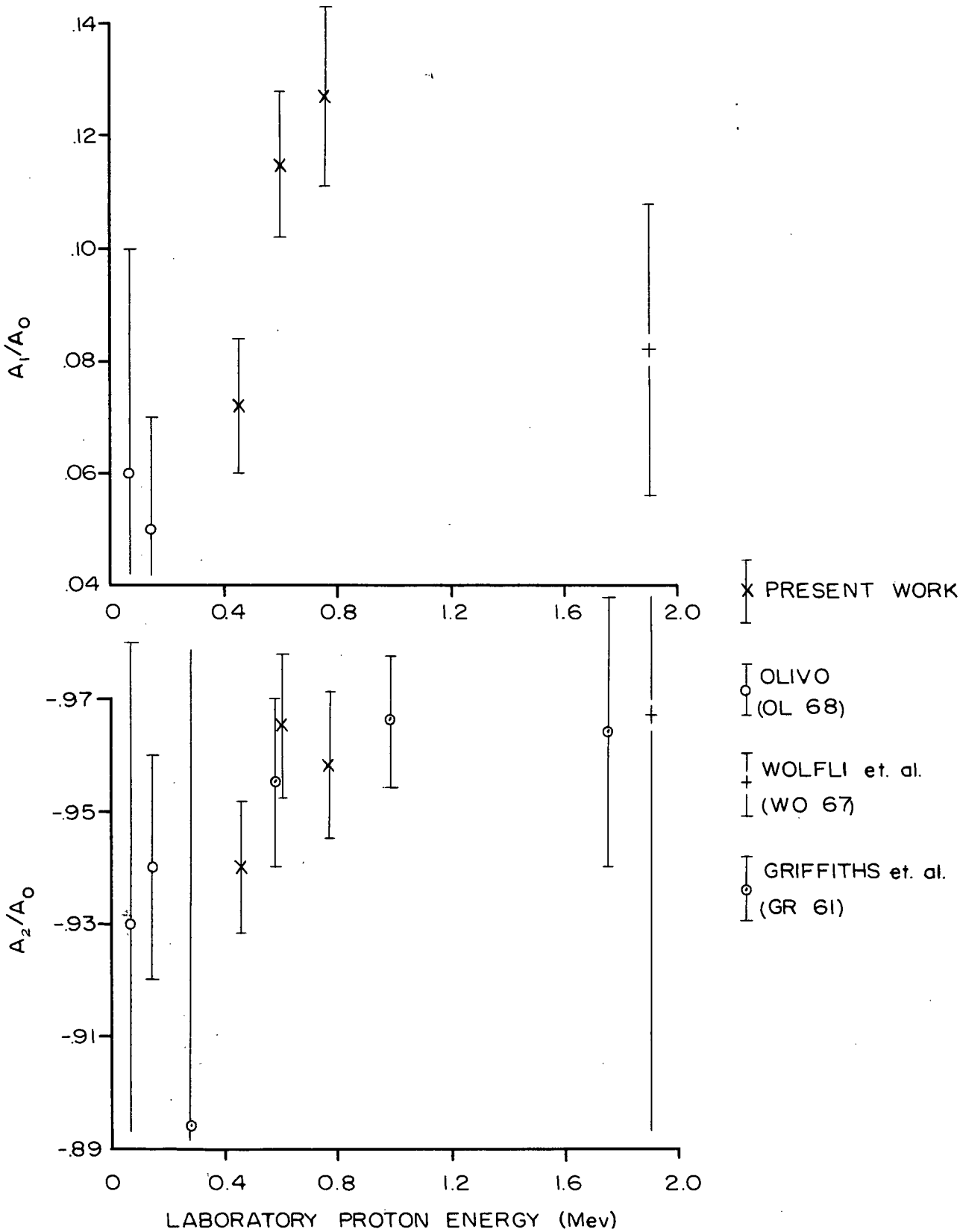

Fig. II-1 : Ratio of the coefficients from angular distribution measurements.

Table II - 2: Smoothing Factors.

Q_1	Q_2	Q_3
.9884	.9655	.9317

Thus the cross section can now be determined, in principle, if the gamma ray yield is measured at 90° to the incident proton beam in an accurately known geometry. But before the description of this measurement, attention will first be focussed on the apparatus used in the experiment, followed by a discussion of the measurement of a series of relative cross-sections, and finally the determination of the gamma detector efficiency, which is required for the computation of the absolute cross section.

CHAPTER III

EXPERIMENTAL APPARATUS

3.1 Target Chamber

The target chamber used for most of the angular distribution runs and for the measurement of the relative cross sections was developed in this laboratory by the author in conjunction with G.M. Bailey and M.A. Olivo. The target consisted of a rotating copper disk covered by a thin layer of deuterated, polyethylene, $(C_2 D_4)_n$. The polyethylene was obtained in powdered form from Merck, Sharp and Dohme of Canada Limited, Montreal, Canada. The chamber was made of brass and the dimensions were approximately eight inches high by six inches in diameter. In order to reduce the gamma ray absorption through the walls of the chamber, the 1/8 inch wall thickness was machined to a thickness of .040 inch in the region over which gamma rays from the reaction could enter the detector.

The target chamber was mounted on an angular distribution table. A lucite insulating disk was attached to the bottom of the chamber, so that the chamber would be isolated electrically from the table. Figure III - 1. shows the chamber and the means of locating it on the table. The nut on the concentric rod attached to the bottom of the chamber enabled the chamber to be raised or lowered.

A lucite insulating ring was placed on the top of the chamber, and the assembly containing the target disk and the motor which rotated it was placed on top of the lucite. Provision was made to water cool the disk to reduce outgassing. The top part could be rotated to place the plane of the disk at any desired angle to the incoming beam.

The gas target which was used for the measurement of the absolute cross section will be described in a later section.

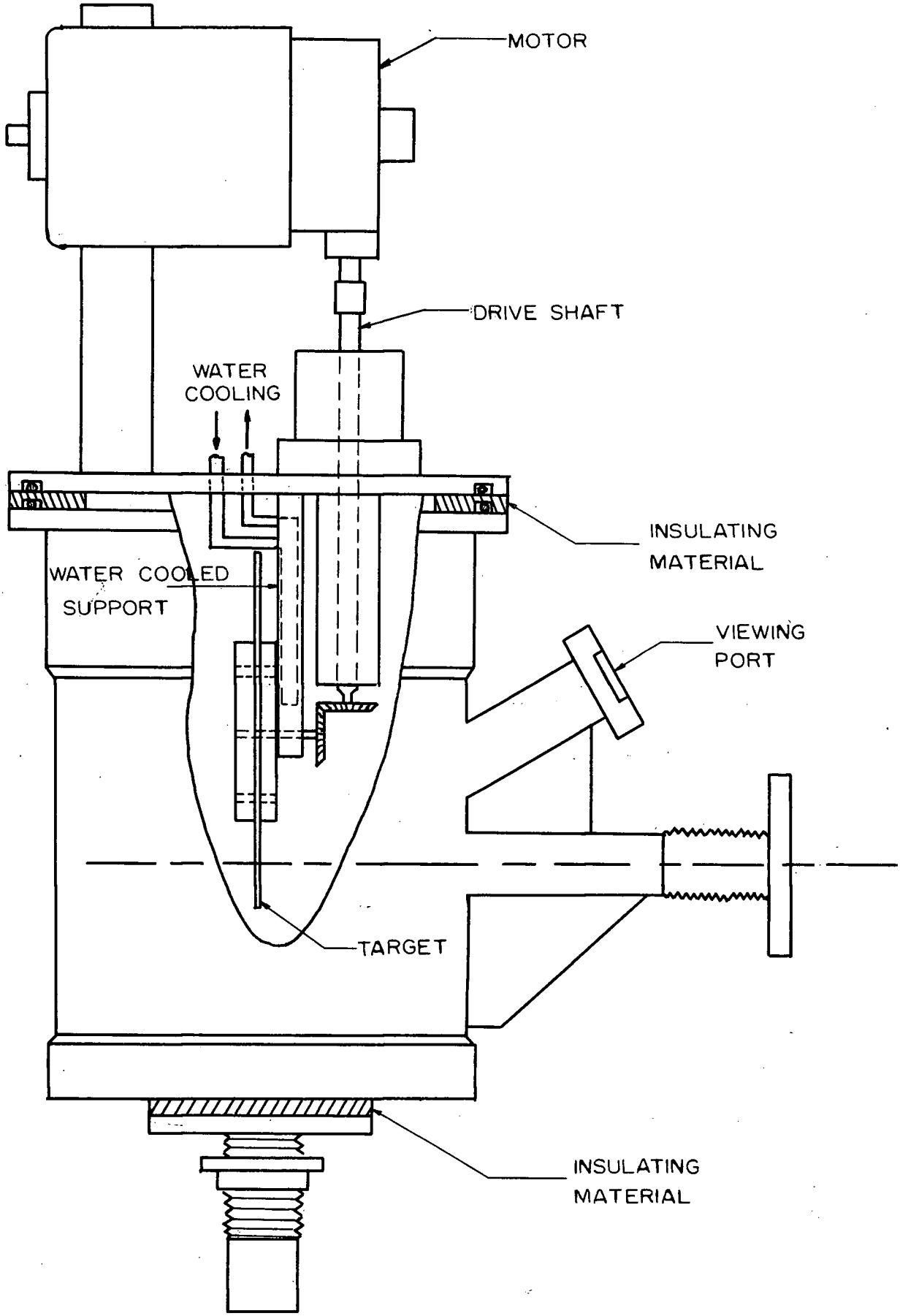

Fig. III-1 : The rotating target chamber.

3.2 Targets

The method of making the targets was as follows. First the deuterated polyethylene was dissolved in xylene by boiling the mixture gently for approximately three minutes. The resultant solution was then poured onto the disk and was prevented from running over the edge by an O-ring which was clamped to the edge of the disk with a metal ring. A smaller O-ring surrounding the central part of the disk limited the deposit to a band about 3 cm. wide. The xylene was then allowed to evaporate slowly at room temperature in a dust free atmosphere, leaving behind a fairly uniform layer of polyethylene.

Note: A superior method of making the targets has since been found and a brief description of this technique follows. The target is machined out of 1/4 inch thick brass leaving two rings of brass to contain the xylene instead of using O-rings for this purpose. The target thickness after machining was approximately 0.066 inches. The disk is then preheated to a temperature at which xylene will boil and the mixture of xylene and polyethylene is then poured into the container and is allowed to boil until all the xylene has evaporated. The disk is finally removed from the heat and is allowed to cool. This method of preparing the target has three distinct advantages. First, the deposited layer of polyethylene is smoother and hence more uniform than was obtained before. Second, there are no losses of the xylene solution through spaces which formerly occurred between the O-ring and the disk, and this method reduces the time taken to make a target from twenty hours to approximately one half hour.

To reduce the background from the copper backing which could be expected at proton energies above approximately 1 Mev, a .001 inch thick platinum

foil was attached to the target base with a high thermal conductivity epoxy (Delta Bond 152, obtained from Wakefield Engineering Inc., Wakefield, Massachusetts) before depositing the polyethylene. The deuterated polyethylene target was rotated while a run was in progress in order to reduce the rate of deterioration.

3.3 Detectors, Collimators, and Shielding.

Two identical 5 inch diameter by 4 inch deep NaI (Tl) gamma ray detectors (HARSHAW type 20 MBS 16/B) mounted on 3 inch photomultipliers (RCA 8054) were used in this experiment.

In order to reduce the background and to keep to a minimum the number of gamma rays scattered into the detectors, they were shielded in the following manner. One, called the D detector during the angular distribution runs, was placed inside a heavy lead shielding, the dimensions of which are shown in Figure III - 2., and listed in Table III - 1. This detector was also shielded by an 8 inch diameter lead collar with a 1 5/8 inch thick wall which fitted over the photomultiplier. Mounted in front of the detector was a lead collimator which limited the acceptance angle for gamma rays coming from the source. This collimator was not used during the relative cross section runs, however; instead a 1/8 inch thick flat lead sheet was placed in front of the detector to reduce the intensity of low energy gamma rays.

The other crystal called the M detector, was placed inside a cylindrical collar with a 1/4 inch thick wall, and was shielded in front by a 1/16 inch thick lead sheet. The back of this detector was shielded by a 1/8 inch thick lead covering which extended over and hence gave further protection to the sides of the crystal.

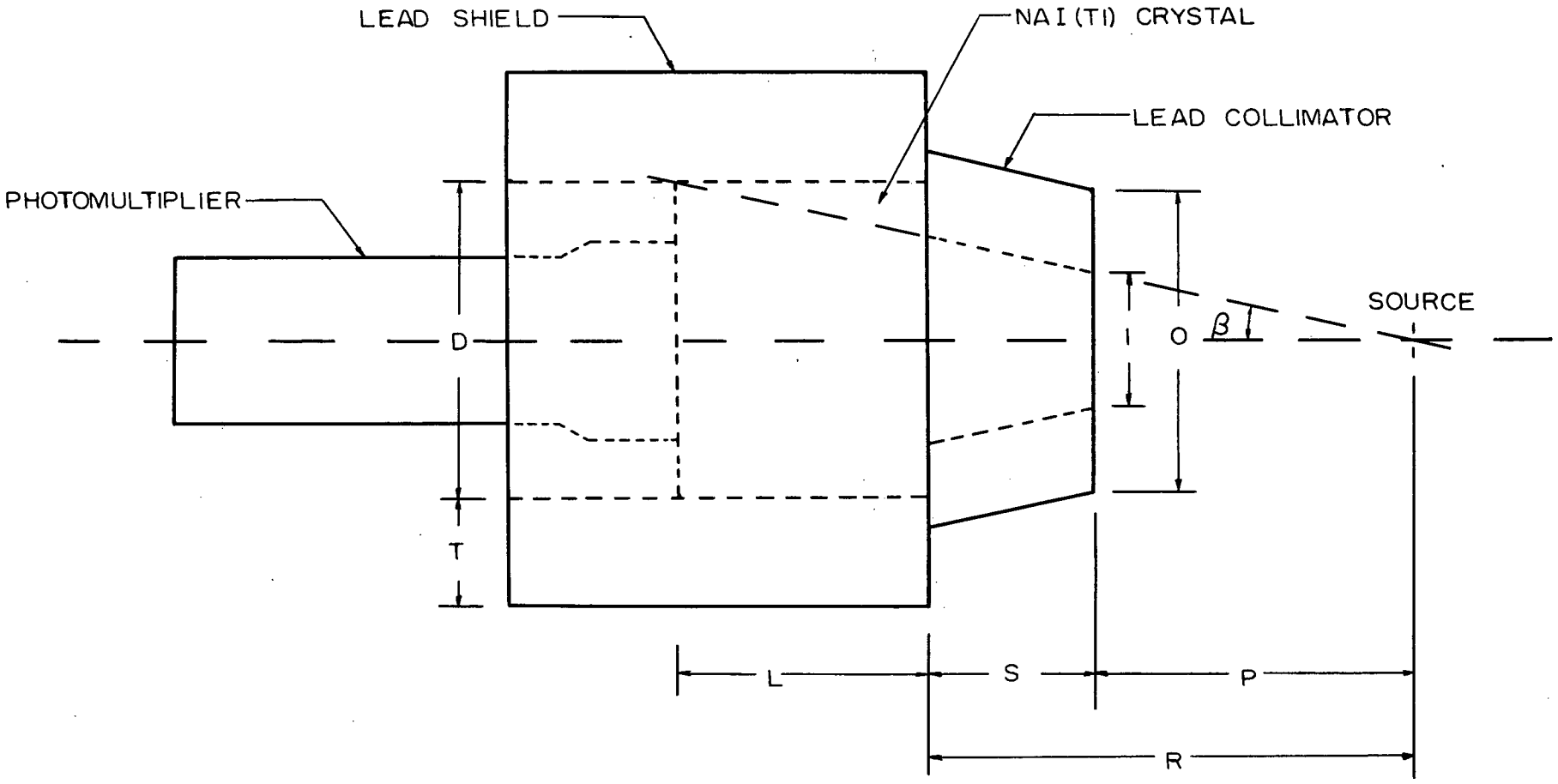

Fig. III-3 : A schematic diagram of the detector assembly. The dimensions are given in Table III-1.

Table III - 1. Dimensions of the D-dector assembly

Collimator Half-angle	β	12.0 ± 0.2	degrees
Source to Crystal Face	R	19.52 ± 0.05	cm
Source to Collimator Face	P	12.46 ± 0.05	cm
Collimator Thickness	S	6.54 ± 0.05	cm
Crystal Diameter	D	12.70 ± 0.02	cm
Crystal Thickness	L	10.16 ± 0.02	cm
Collimator Face Inner Diameter	I	5.30 ± 0.05	cm
Collimator Face Outer Diameter	O	11.6 ± 0.1	cm
Thickness of Lead Shielding	T	4.0	cm

3.4 Electronics

The electronic equipment used in the experiment is discussed in some detail in the section to which a particular configuration is relevant. Circuit diagrams of the photomultipliers and preamplifiers for the detectors have previously been presented (OL 68). A complete list of the electronics used during the experiment is given in Table III - 2. The numbers in parentheses in the block diagrams refer to the numeral order in Table III - 2.

3.5 Data Analysis

Several computer programs were written for the U.B.C. IBM 7044 computer to assist in the analysis of the data. The rather complex analysis procedure was required in order to separate from the gamma ray spectra background radiations falling in the same energy range as the $D(p,\gamma)^3He$ gamma rays. The main contributions to this background were 6 and 7 Mev gamma rays from the reaction $^{19}F(p,\alpha\gamma)^{16}O$, and 8 Mev gamma rays from the reaction $^{13}C(p,\gamma)^{14}N$

A list of the computer programs, with a brief description of each, is given in the Appendix.

3.6 Proton Beam

The proton beam was obtained from the U.B.C. Van de Graaff accelerator. This machine is capable of delivering a beam of approximately 20 microamps on target for the energy range covered during this experiment.

TABLE III- 2 : List of the electronic units used in this experiment

1. FLUKE Model 412-B High Voltage Power Supply
2. HARSHAW Type 20MBS16/B 5" x 4" NaI(Tl) crystal coupled to an RCA 8054 3 inch photomultiplier
3. U. B. C. Power Supply
4. U. B. C. Preamplifier
5. U. B. C. Pulse generator
6. NUCLEAR DATA ND-160 Dual Parameter Analyzer
7. NUCLEAR DATA ND-120 Pulse Height Analyzer
8. NUCLEAR DATA ND-500 Dual Amplifier and Single Channel Analyzer
9. ORTEC Model 430 Scaler
10. ORTEC Model 210 Detector Control Unit
11. RCA Type C-3-75-0.2 Diffused Junction Detector
12. ORTEC Model 101 Low Noise Preamplifier
13. ORTEC Model 201 Biased Amplifier
14. CANBERRA INDUSTRIES Model 1410 Linear Amplifier
15. FLUKE Model 881A DC Differential Voltmeter
16. ELECTRO SCIENTIFIC INDUSTRIES Model 250 DE Impedance Bridge
17. ELECTRO SCIENTIFIC INDUSTRIES Model 300 Potentiometric Voltmeter-Bridge
18. ELDORADO ELECTRONICS Model CI-110 Current Integrator

CHAPTER IV

RELATIVE CROSS SECTION MEASUREMENTS

4.1 Experimental Apparatus

The absolute cross section measurement was made with a gas target which could only take a small amount of beam and therefore required a long run. To measure cross sections at all energies with this target would have required a very long time. Thus it was decided to determine the relative yield of the reaction at several energies from 400 kev to 1100 kev with the deuterated polyethylene target, and then to measure the absolute cross section at only one energy, thereby effectively determining the absolute cross section over the entire energy range explored. The target was prepared as discussed in the previous chapter, and its thickness was estimated to be approximately 50 micrograms per cm^2 corresponding to an energy loss of 14 kev for 800 kev incident protons. The rotating disk was set at an angle of 45° to the incoming beam as shown in Figure IV - 1. Also shown in this figure are the two detectors placed at 90° to the incoming beam, which were shielded in the manner discussed in the last chapter. The distance from the target centre to the crystal face was $4\frac{1}{2}$ inches.

The rotating disk was electrically connected to the rest of the target chamber so that electrons which were ejected from the target by secondary emission caused by the incoming protons would not cause an error in the measurement of the current, since these emitted electrons would eventually reach the chamber walls. There would also be some protons scattered off the target to the walls and this electrical tieup insured that these protons would also be measured. The current was integrated by an Eldorado Electronics Current Integrator, Model CI-110, which was checked for leakage current at the completion of the run.

A block diagram of the electronics used is shown in Figure IV - 2.

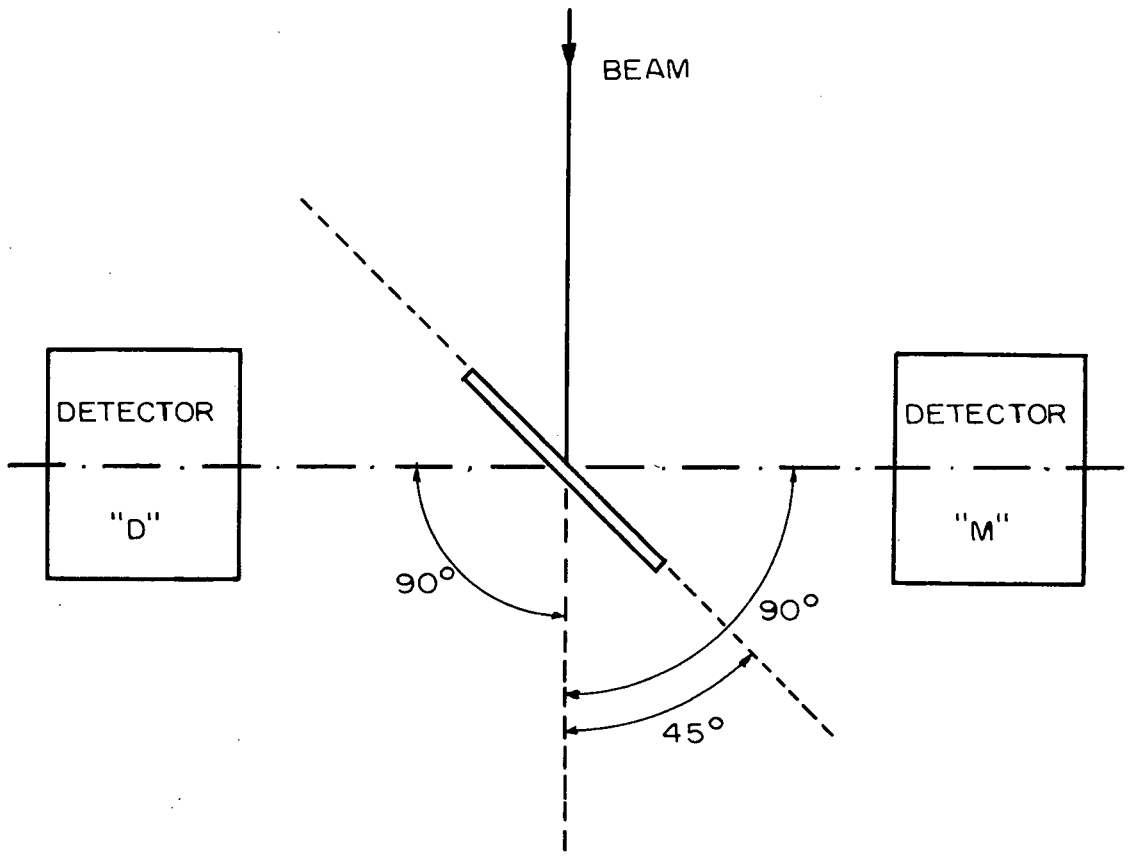

Fig. IV-1 : Detector target configuration for the relative cross section runs.

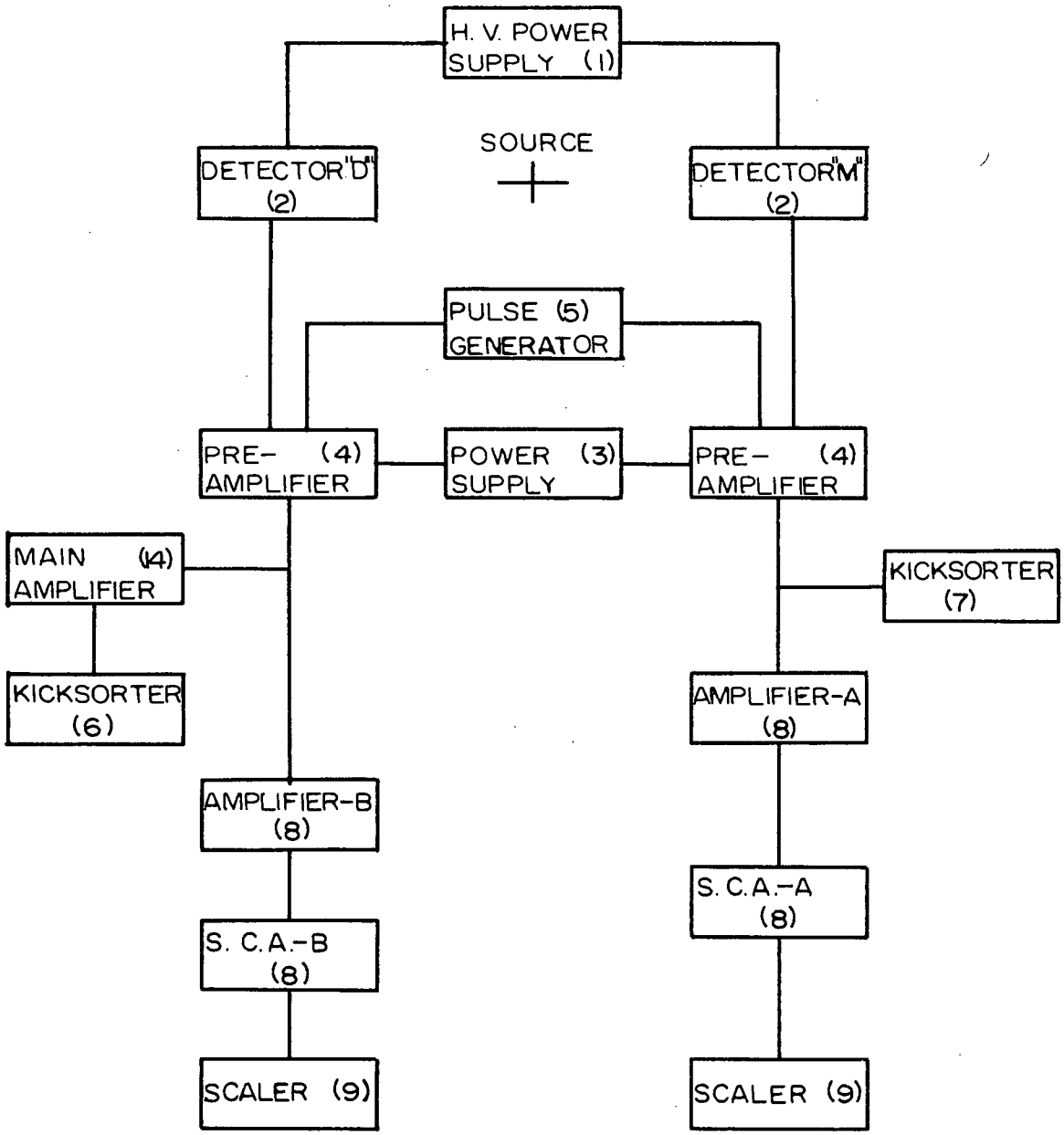

Fig. IV-2 : Block diagram of the electronic arrangement for the relative cross section runs.

The pulse generator was used to check the linearity of the kicksorter and for setting the windows on the single channel analyzers. The scalers were used to monitor the deterioration rate of the target, but were not used at all in the analysis of the data.

4.2 Procedure

It was known that the target would decay appreciably during the runs so it was necessary to constantly remeasure the yield at one particular energy so that the yield at other energies could be normalized to this. These normalization measurements were taken at a proton laboratory energy of 800 kev, and the other measurements were taken at proton energies of 400 kev, 470 kev, 520 kev, 620 kev, 700 kev, 1000 kev, and 1100 kev. All the runs were taken for an integrated charge of from 6000 to 22,500 microcoulombs.

The data was analyzed by the method discussed in the next section.

4.3 Data Analysis and Results

Rather than add together the data collected by the two detectors and determine the relative yield from this, it was decided to analyze the results separately, thereby determining a relative yield curve for each detector. These two yield curves were then blended together to obtain the relative yield at the various energies. The two sets of data are referred to as the M crystal and D crystal results.

The spectra were first gain-shifted to a standard gain and zero by the computer program TREAT. This program was also used to subtract a time dependent room background from the data. The modified data was then processed by NAILS, a complex analysis program, which analyzed the data into a specified set of components. From this, one could determine the number of gamma

rays in the spectrum which originated from the $D(p,\gamma)^3He$ reaction. A typical output of the NAILS program is shown in Figure IV - 3, which gives the ratio of the number of counts in a preselected range of the spectrum introduced by various components as listed (M6.224 gives $D(p,\gamma)^3He$ component, F19MHI gives $^{19}F(p,\alpha\gamma)^{16}O$, C135M gives $^{13}C(p,\gamma)^{14}N$, NBGSM gives neutron background, and M4.439 gives $^{15}N(p,\alpha\gamma)^{12}C$). The curve shows the total spectrum fitted to the data.

The spectrum represented in this figure is for a proton bombarding energy of 1100 kev. From the relative intensities listed, it is clear that a considerable amount of the spectrum arose from gamma rays originating from the other reactions, and from the neutron background which arose partly from D on D knock-on reactions in the target and partly from D on D reactions in the magnet box.

The number of gamma rays from the $D(p,\gamma)^3He$ reaction was corrected for dead time losses in the kicksorter, and for absorption of gamma rays by the target backing, this latter correction being applied only in the case of the D crystal results.

Now it was necessary to normalize all the results to a given target thickness since the target was decaying while the runs were in progress. In order to monitor this decay, several repetition runs were made at a proton energy of 800 kev. The results of these runs are shown in Figure IV - 4. The yields shown were those obtained from the analysis as described so far. The error bars indicate the statistical uncertainty resulting from the number of counts. A small correction was added to allow for errors in the computer program NAILS (part of the output of this program was an estimate of the error). The fourth run was omitted as being inconsistent with the rest. Probably the beam spot shifted during this run.

It is seen that the M crystal yield is about 20 percent higher than

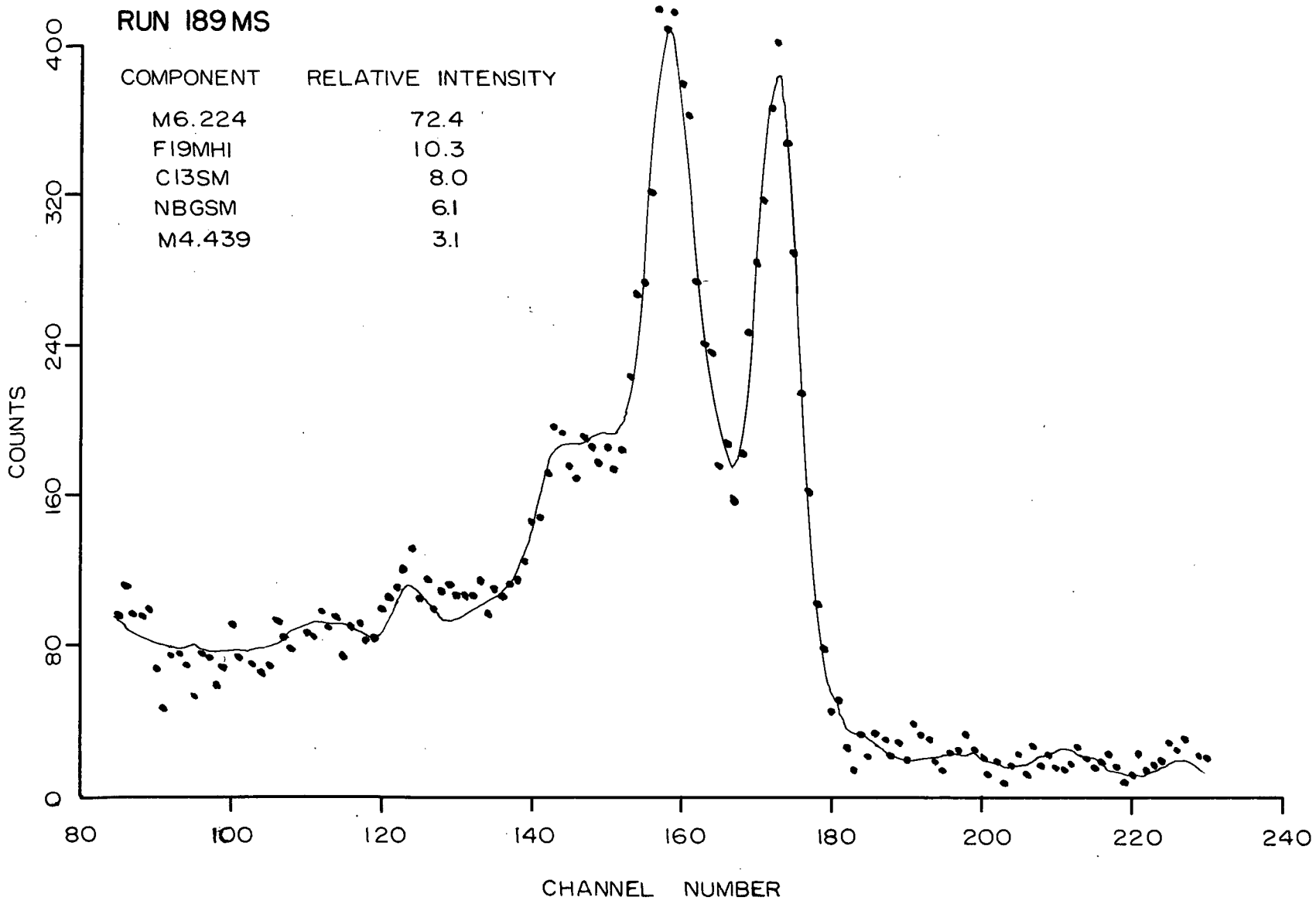

Fig. IV-3 : Typical spectrum after analysis by the NAILS computer program.

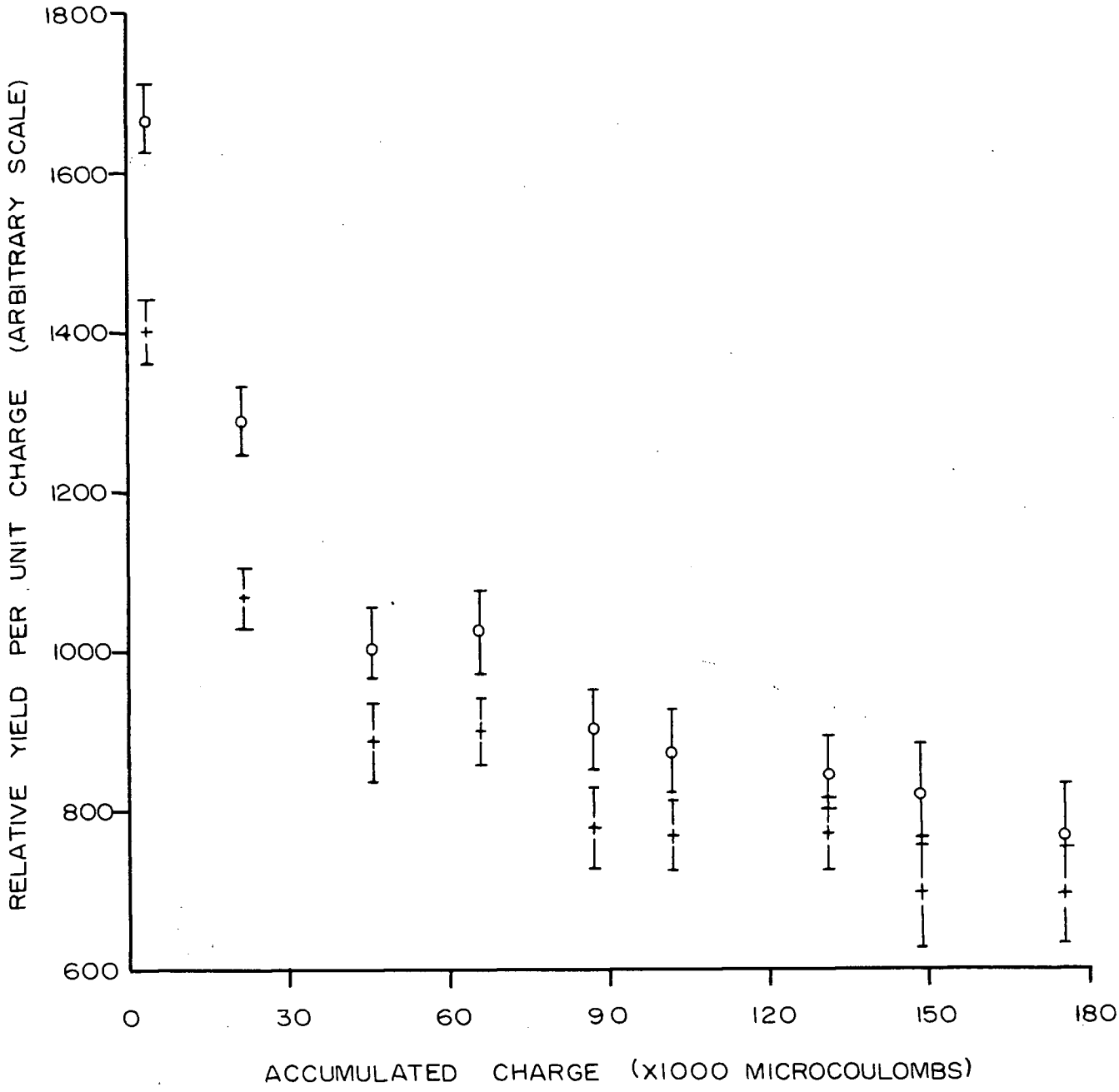

Fig. IV-4 : Target decay from the 800 kev runs.
The circles refer to the M crystal.
The crosses refer to the D crystal.

the D crystal yield. This is the result of the more scanty shielding of the M crystal, and of the absorption of gamma rays by the target backing which affected only the D crystal.

The results of the normalization runs were fed into the computer program POLY-D, which fitted each curve separately as the sum of two exponentials. The yield per unit charge for each of the relative cross section runs was then determined and the counts obtained for each run were multiplied by the appropriate amount to allow for the target decay. A small correction was also applied to allow for the efficiency change of the detectors with the changing energy of the gamma ray.

The result of this normalization procedure was to obtain relative cross section curves, one for the D crystal and one for the M crystal. These curves are shown in Figure IV - 5.

The error bars indicate partly the statistical error resulting from the number of counts. This was typically of the order of 3 percent. Again, a small amount was added to this to allow for errors in the computer program NAILS. The rest of the error results from an uncertainty of about 3 percent in the target decay. The root mean square sum of these errors was approximately 5 percent.

The two results were then blended together in the following way. First, each set of results was fitted with a cubic least squares curve. The D curve was then multiplied by a constant factor to give the best fit with the M curve. This analysis was done with the computer program CSFIT. A small correction was then applied to allow for the change of the angular distribution with energy. The resultant relative cross section curve is shown in Figure IV - 6.

The errors arise from two sources. First, there is the error outlined above for the results from each crystal. Added to this is a 1 percent error for the blending procedure done by CSFIT. The total error then is

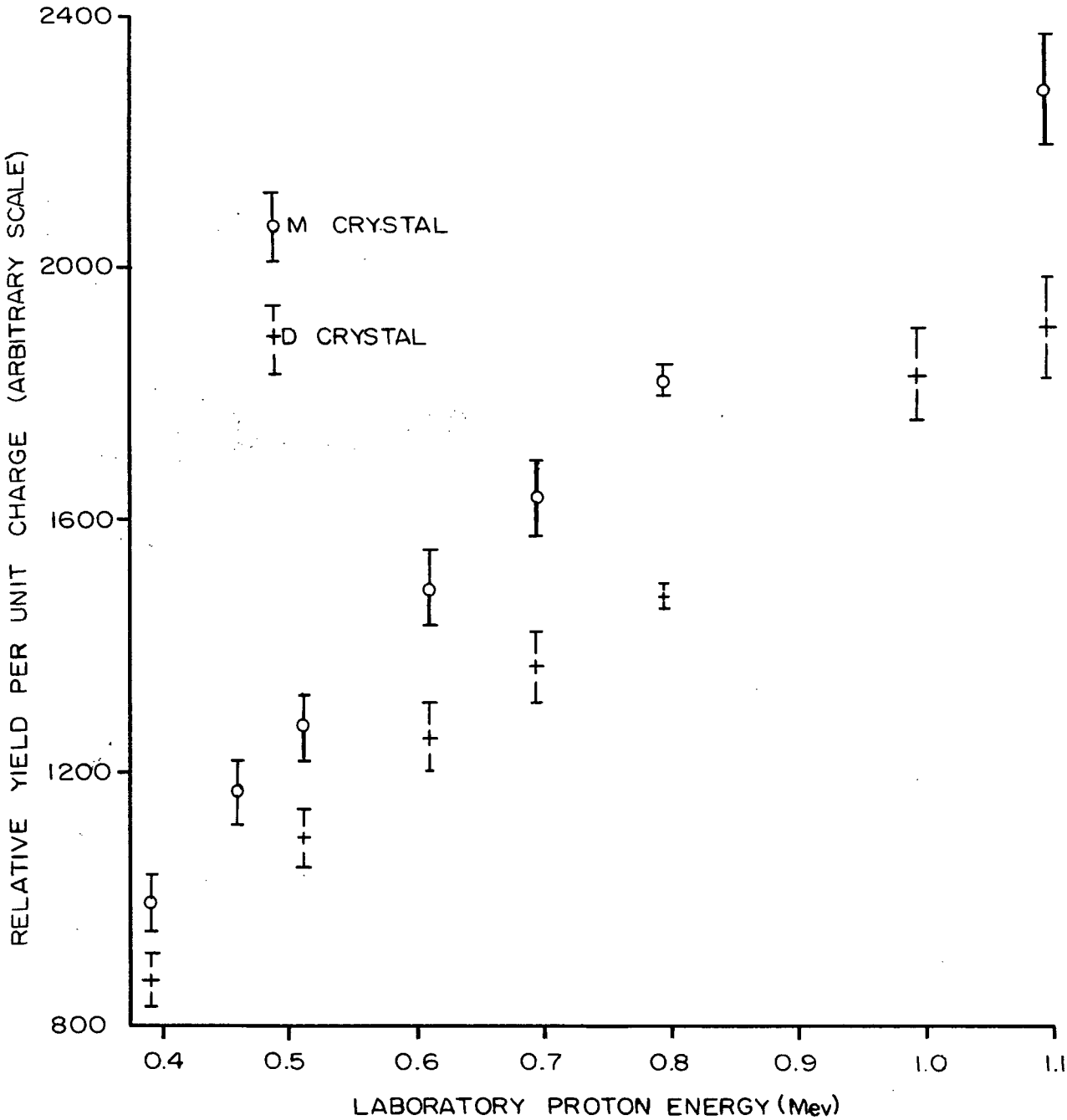

Fig. IV-5 : Relative yield curve obtained for each detector.

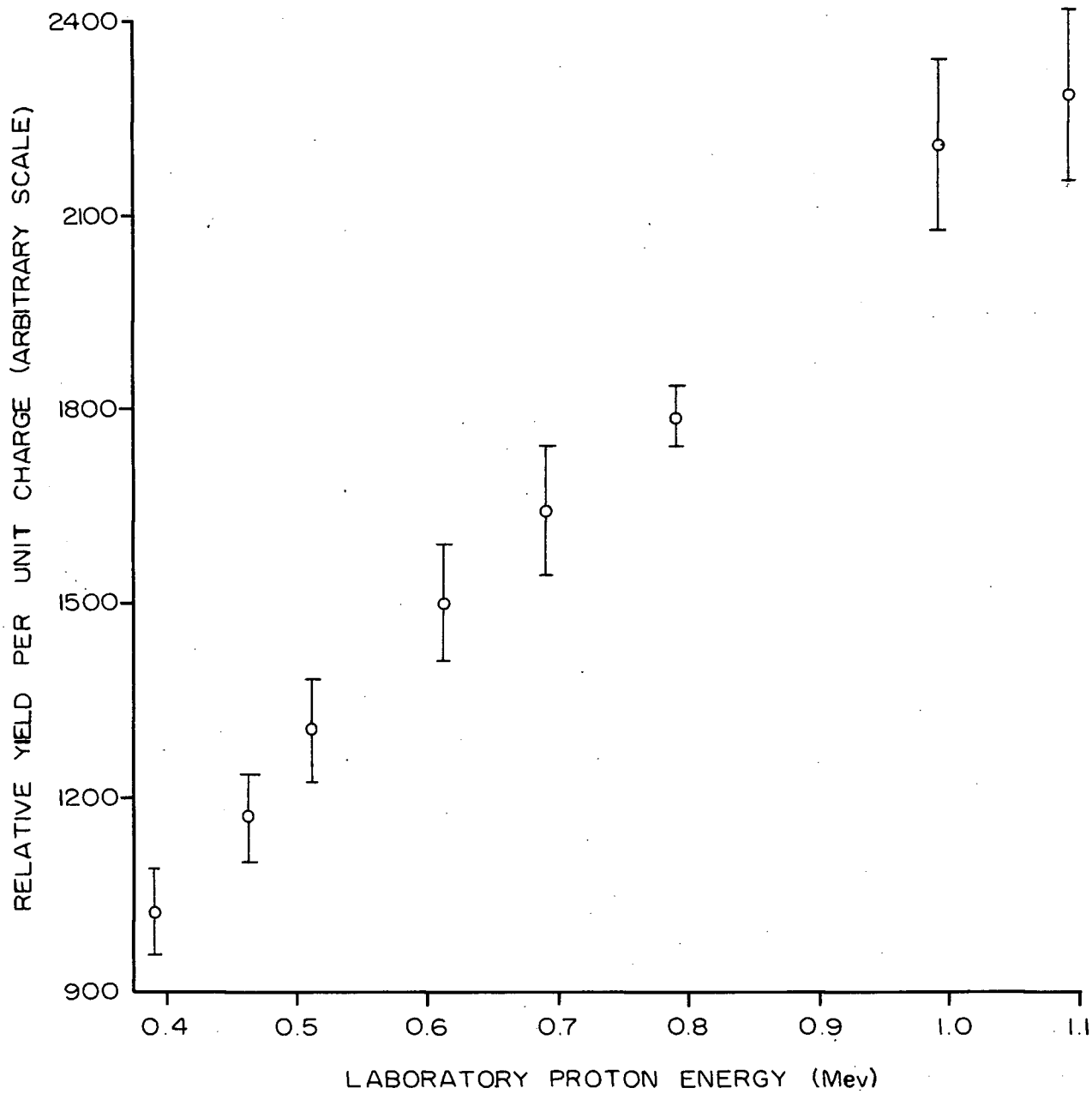

Fig. IV-6 : Relative yield for the reaction $D(p,\gamma)^3He$.

approximately 6 percent.

With this section of the work completed, it now remained only to fix the location of the curve by measuring the absolute cross section. Before this could be done, however, it was necessary to determine the crystal efficiency, which is the subject of the next chapter.

CHAPTER V

EFFICIENCY MEASUREMENTS

5.1 Introduction

It was necessary to determine an accurate detection efficiency of the scintillation counters for gamma rays before the absolute cross section could be obtained. The reaction $^{19}F(p,\alpha\gamma)^{16}O$ was utilized for this purpose. In this reaction the protons can be captured by ^{19}F at several resonances to form excited states of ^{20}Ne, which subsequently decay by alpha emission to the ground state of ^{16}O (α_0), or to one of the excited states of this nucleus. These latter states are the 6.06 Mev state (α_π), which decays by electron pair emission to the ground state, the 6.14 Mev state (α_1) the 6.91 Mev state (α_2) and the 7.12 Mev state (α_3) which all decay by gamma ray emission to the ground state. It has been shown (FR 50) that for the 340 kev resonance where the present measurements were made, the ratio of $\frac{\alpha_2 + \alpha_3}{\alpha_1}$ is 0.024. It has also been found that at 340 kev bombarding energy, the alpha decay to the ground state (α_0) and to the pair emitting state (α_π) were not experimentally observable (CH 50). This same experiment showed that the number of alpha particles emitted was in close agreement with the number of gamma rays, and that the angular distribution of both reaction products was isotropic. Devons and Hine (DE 49) had previously shown that the gamma rays were isotropic.

The foregoing discussion implies that to determine the efficiency of a gamma ray detector of a specified geometry one has only to measure the number of alphas emitted into a known geometry. One can then get the efficiency as the ratio of the number of gamma rays detected to the number of alphas detected, after suitably correcting for the different geometries of the two detectors.

That is to say, the efficiency is $\varepsilon = \frac{N_\gamma \omega_\alpha}{N_\alpha \omega_\gamma}$

where ε is the intrinsic efficiency and

N_γ is the number of gamma rays detected

N_α is the number of alphas detected

ω_α is the solid angle subtended at the source by the alpha counter

ω_γ is the solid angle subtended at the source by the gamma detector.

5.2 Apparatus

(a) Target Chamber

The target chamber used for the efficiency measurements (Figure V-1) has been used previously in this laboratory (LE 64) for the same purpose. The original alpha detector had been destroyed, however, and so this was replaced by one of similar dimensions. The characteristics of the alpha detector (RCA diffused junction detector type C-3-75-0.2) are listed in Table V-1.

TABLE V-1: Properties of the alpha detector

Material	Phosphorus diffused into n-type silicon
Resistivity	1000 ohm-cm
Diffusion Depth	0.2 microns
Sensitive Area	20 mm^2
Operating Voltage	20 volts
Leakage Current (measured)	0.43 microamps
Resolution (5.13 Mev alphas)	107 kev

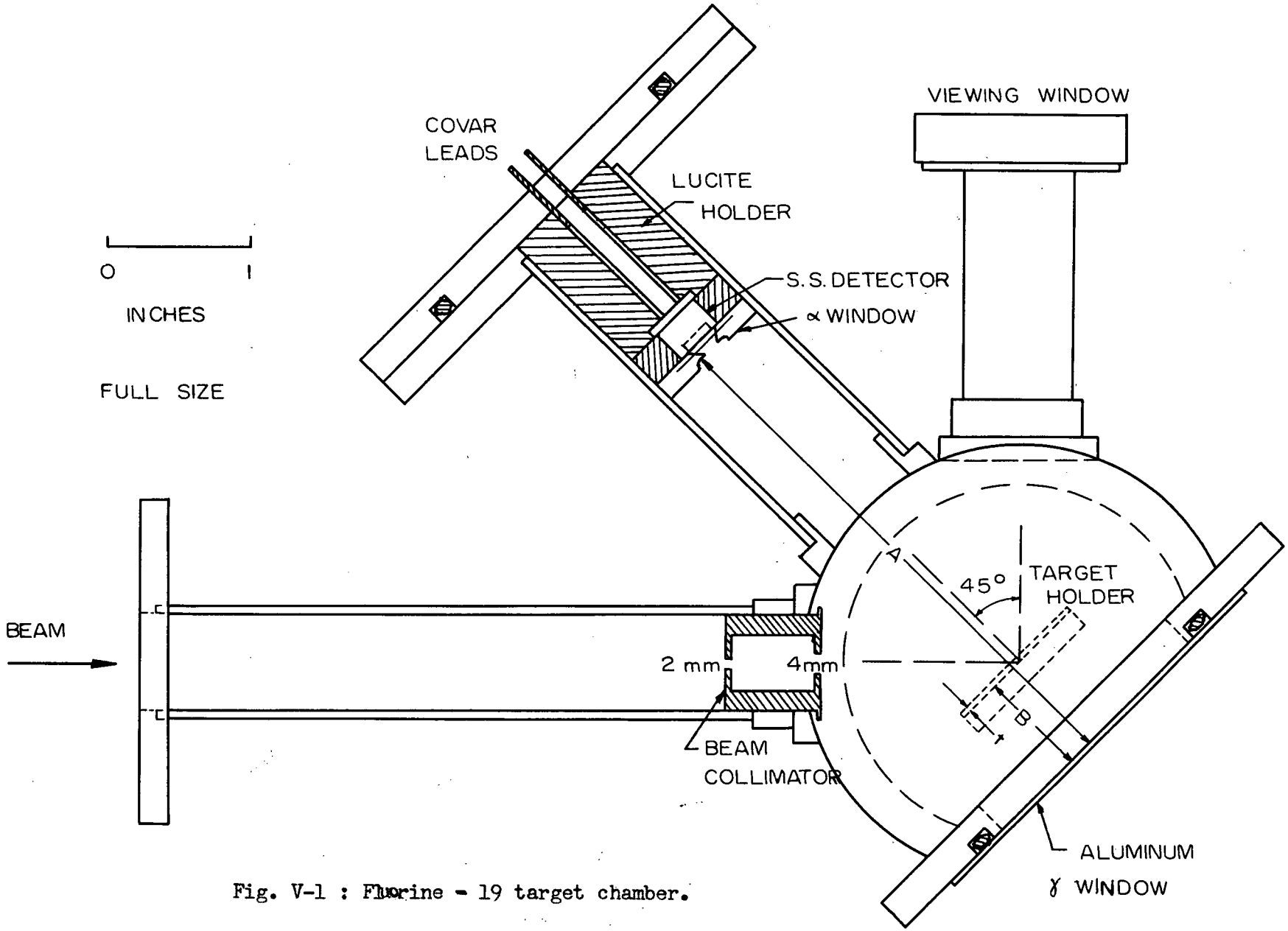

Fig. V-1 : Fluorine - 19 target chamber.

A 25 micro-inch sheet of Grade C (pinhole free) nickel foil obtained from the Chromium Corporation of America was placed in front of the alpha detector in order to reduce the scattered proton flux which would otherwise enter the detector at a similar energy to the alphas. This nickel window also reduced the energy of the α_2 and α_3 particles, so that these now appeared in the same region as the scattered protons. The entrance window to the alpha detector is shown in detail in Figure V- 2.

The target chamber was aligned making use of the angular distribution table on which it rested, and the gamma detector collimator, which had cross wires mounted on the front and back. These cross-wires were placed in such a way as to accurately define the centre of the collimator. One then aligned the centre of the beam entrance collimator with the previously mentioned cross-wires; then the angular distribution table was rotated to check that the line joining the centre of the entrance window to the alpha counter was in line with the cross-wires. This ensured that the axis of both detectors passed through the centre of the beam spot on the target.

(b) Fluorine Targets

The requirements for a satisfactory target is that it must be thin enough to allow the alphas to escape and the protons to pass through without too much degradation of energy, and thick enough to get a reasonable yield. For 340 kev bombarding protons, this means that a thickness of approximately 5 to 10 kev would be sufficient.

Following the procedure used by Larson (LA 57) in this laboratory, the targets were made by evaporating powdered calcium fluoride onto thin copper plates. The method is to put the CaF_2 in a tantalum boat and pass through this a large current while the apparatus is under vacuum (approximately 10^{-5} mmHg). The vapour then deposits on the copper plates which are placed above the boat.

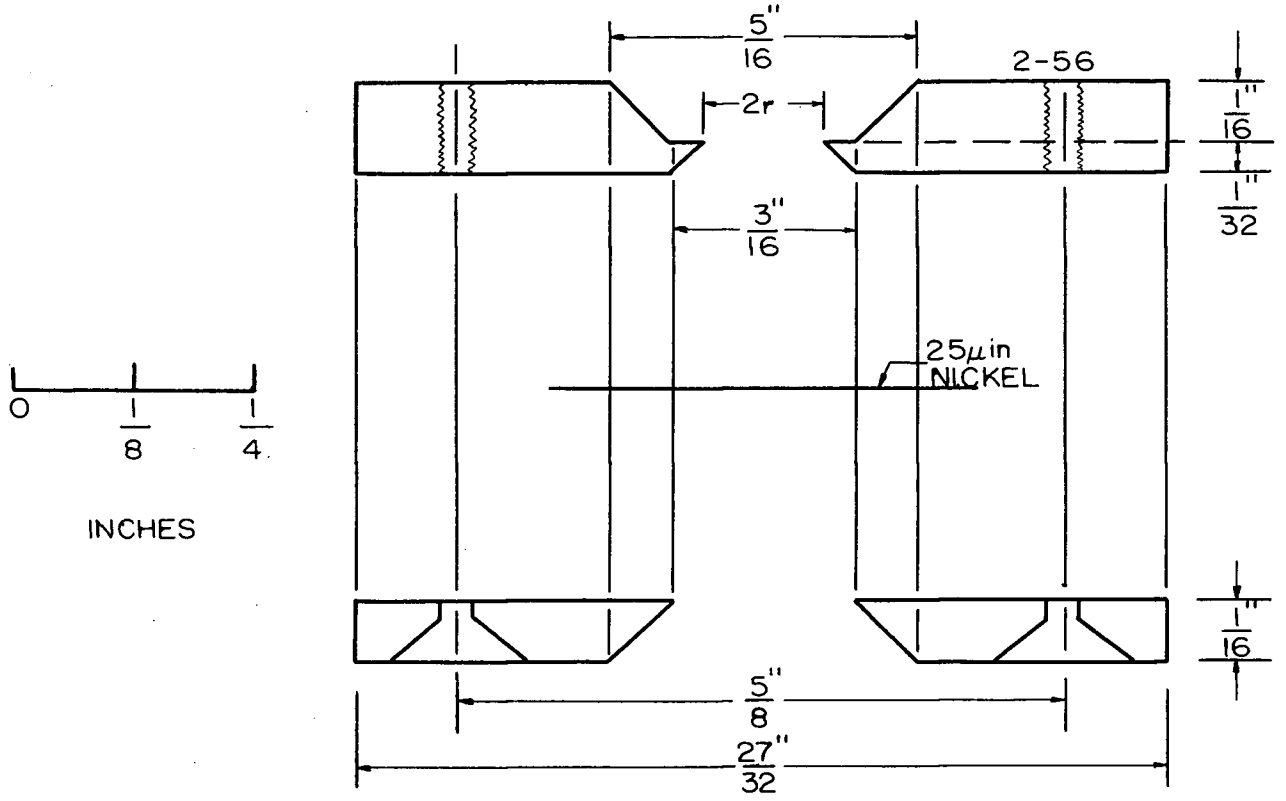

Fig. V-2 : Alpha particle window.

The stand holding the plates was arranged so that two targets could be made at one time, each at a different distance above the boat. Three pairs of targets were made in this fashion, varying each time the amount of CaF_2 placed in the boat. Six targets of different thicknesses were thus obtained.

The targets were then mounted in the chamber, one at a time, to determine their thicknesses to 340 kev protons. To ensure that the target was at an angle of 45° to the beam direction a micrometer depth gauge was clamped onto the back of the chamber, and the feeler rod was screwed in until it just touched the back of the target. The target was then rotated until the rod and its reflection in the target formed a straight line. Since the back of the chamber was 45° to the beam direction, the target then was also oriented this way. The excitation function is shown in Figure V-3 for the target selected. The thickness at half maximum was approximately 7 kev.

(c) Alpha Detector Electronics

Pulses from the alpha detector were fed into an Ortec Model 101-201 Low Noise Preamplifier-Amplifier combination, and from there into 512 channels of a Nuclear Data Type 160 1024-channel kicksorter. The alpha particle pulses were also fed to a single channel analyzer and scaler in order to monitor the number of alphas during the run.

A block diagram of the electronics (including the gamma detection circuit) is given in Figure V-4. A description of each unit appears in Chapter III.

The kicksorter was calibrated with 5.13 Mev alphas from a ^{239}Pu source which was inserted into the target chamber for this purpose. The spectrum thus obtained is shown in Figure V-5. Since the energy of the alphas from the reaction is only 1.73 Mev in the laboratory system, the gain of the main amplifier was halved after calibrating the kicksorter, so that the alpha spectrum from the

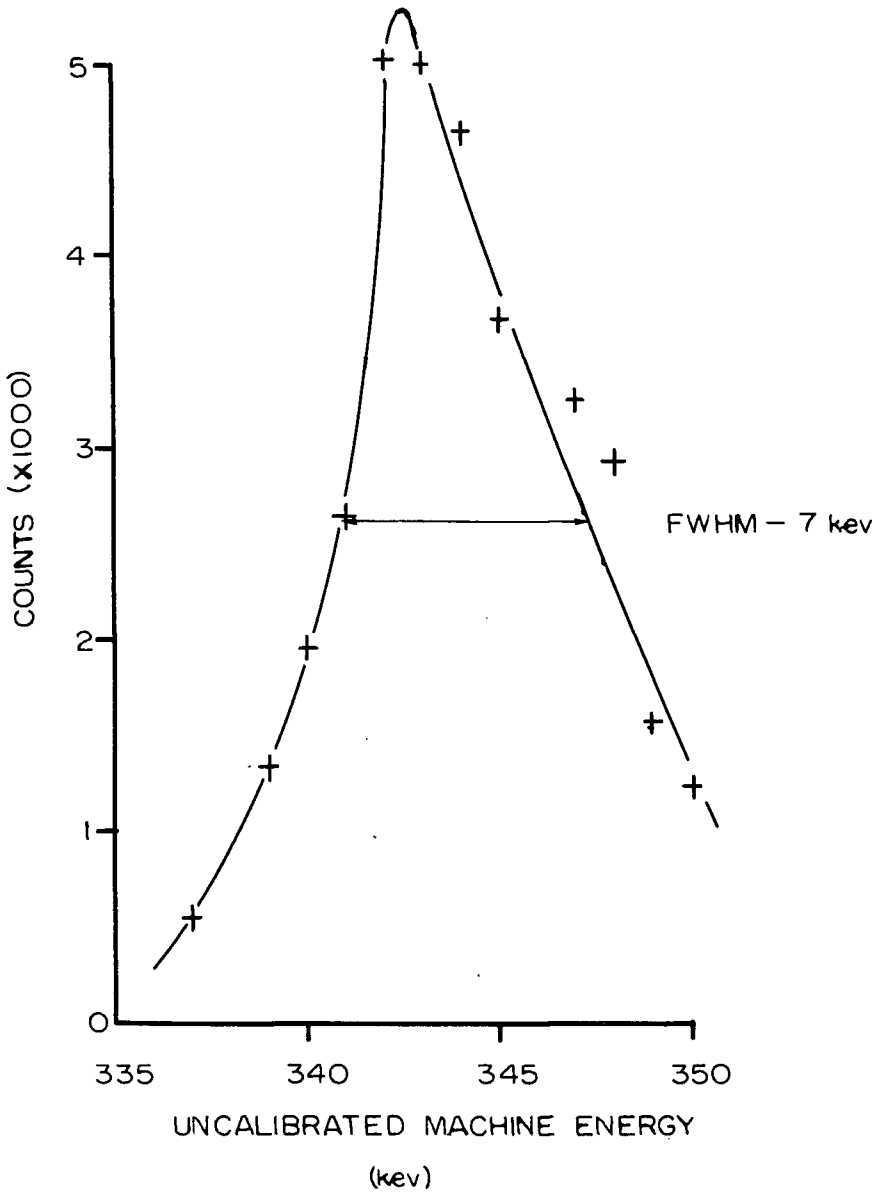

Fig. V-3 : Excitation function for ^{19}F target used for the efficiency measurements.

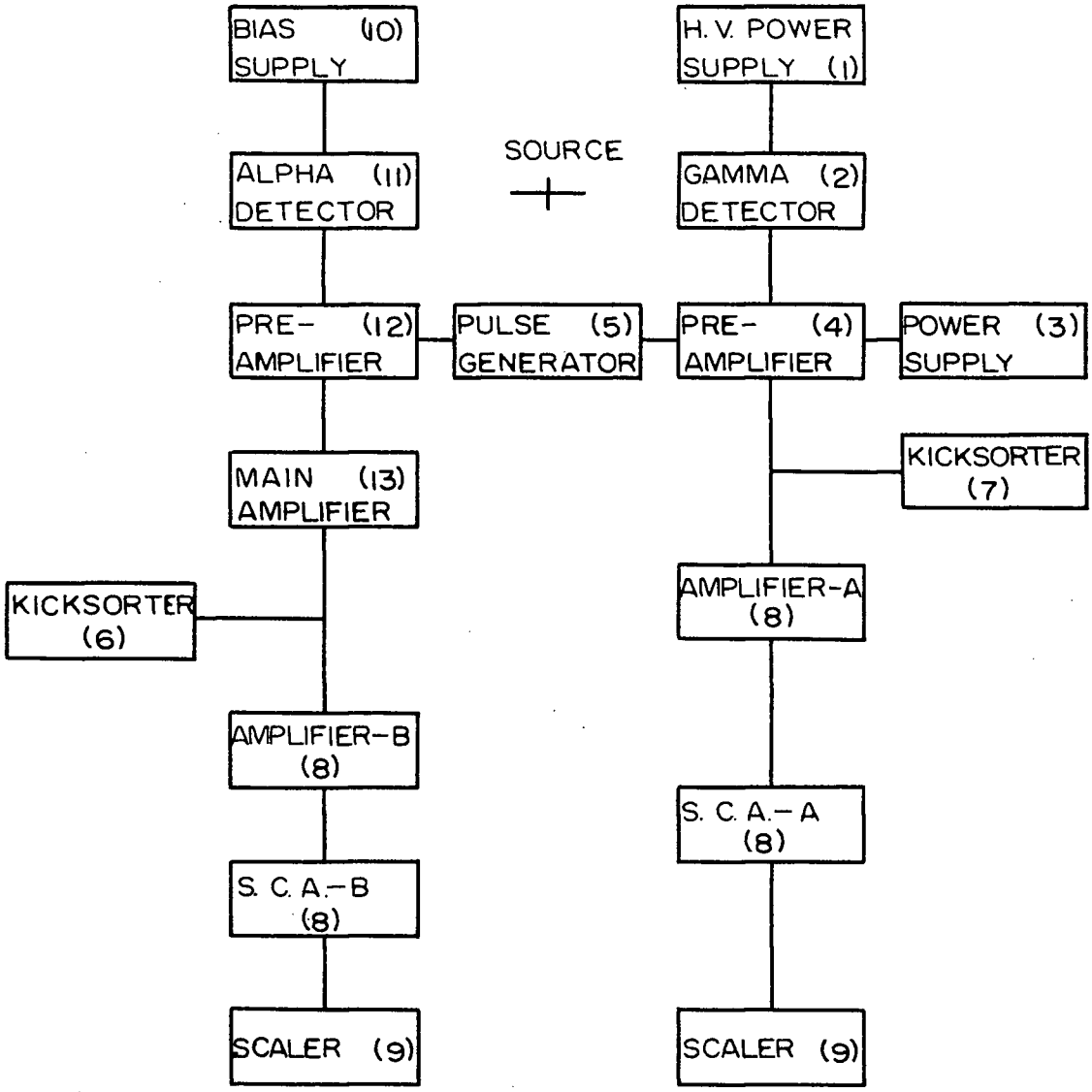

Fig. V-4 : Block diagram of the electronic arrangement for the crystal efficiency measurements.

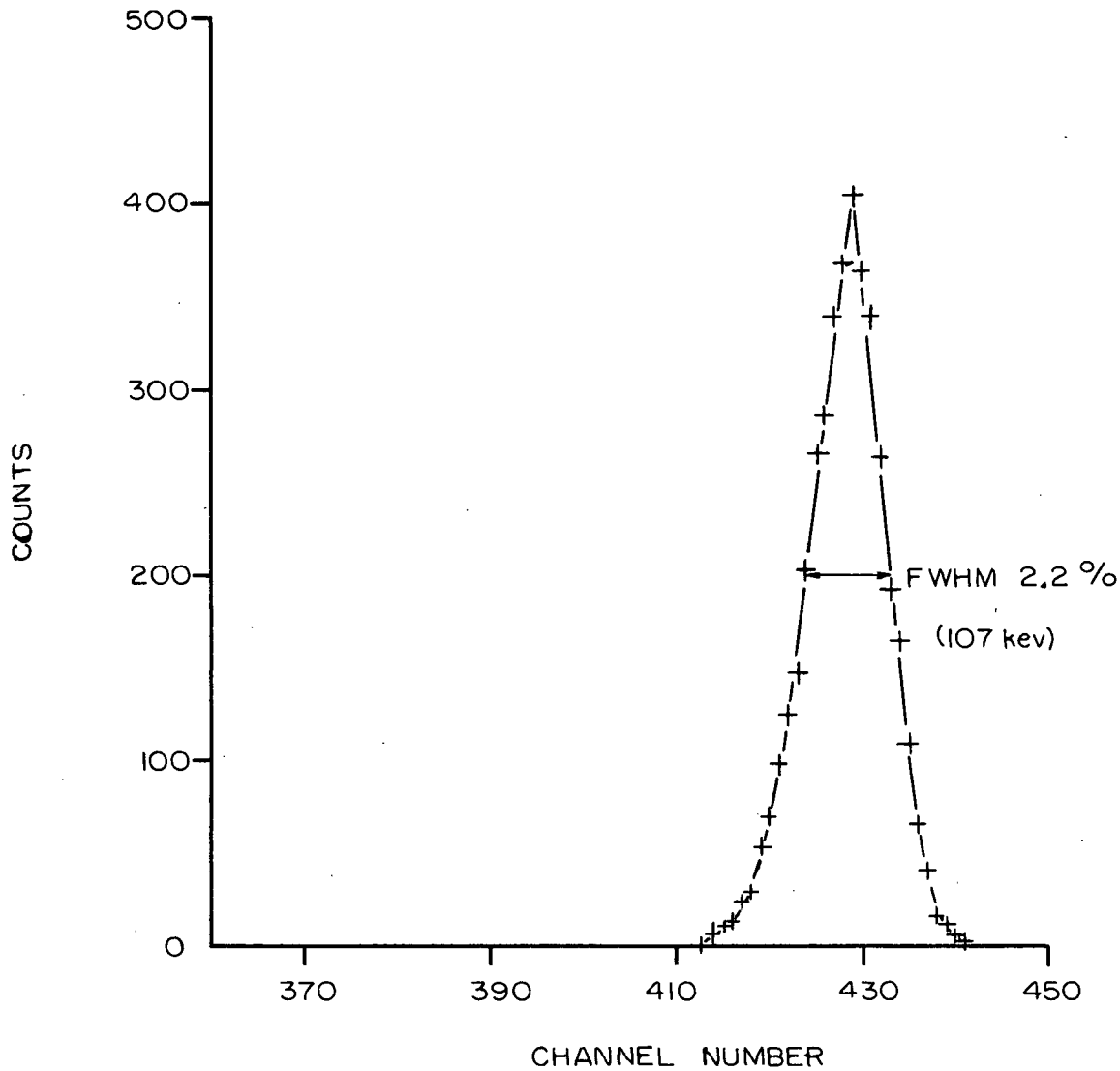

Fig. V-5 : 5.13 Mev ^{239}Pu alpha particle spectrum.

reaction would be more nearly in the centre of the range. Finally the linearity was checked using the pulser, and this was found to be excellent over the entire range. A typical alpha spectrum from the $^{19}F(p,\alpha\gamma)^{16}O$ reaction is shown in Figure V - 6.

(d) Gamma Detector Electronics

The pulses from the gamma detector were fed into a preamplifier and then directly into the ND 120 kicksorter. A single channel analyzer and scaler were also used so that a continuous check could be made on the number of gamma rays being detected and hence on the deterioration of the target. A typical gamma spectrum from the reaction is shown in Figure V - 7.

5.3 Solid Angle Calculations

(a) Alpha Detector

The alpha detector is mounted so that it detects particles at 135° to the incident proton beam and 90° to the target face. The relevant geometry for the calculation of the solid angle is displayed in Figures V - 1 and V - 2, and the dimensions shown there are listed in Table V - 2.

Table V - 2: Alpha detector solid angle

Distance Measured		Method of Measurement
Window diameter (2r)	$3.196 \pm .001$ mm	Travelling microscope over 15 diameters
Distance A	$3.9836 \pm .001$ in	Precision depth gauge
Distance B	$.7225 \pm .0001$ in	Precision depth gauge
Target backing t	$.0115 \pm .0001$ in	Micrometer
Detector Window to Target Face R = A-B-t	$3.2496 \pm .0002$ in	
Solid Angle (calculated)	$(1.18 \pm .01) \times 10^{-3}$	steradians

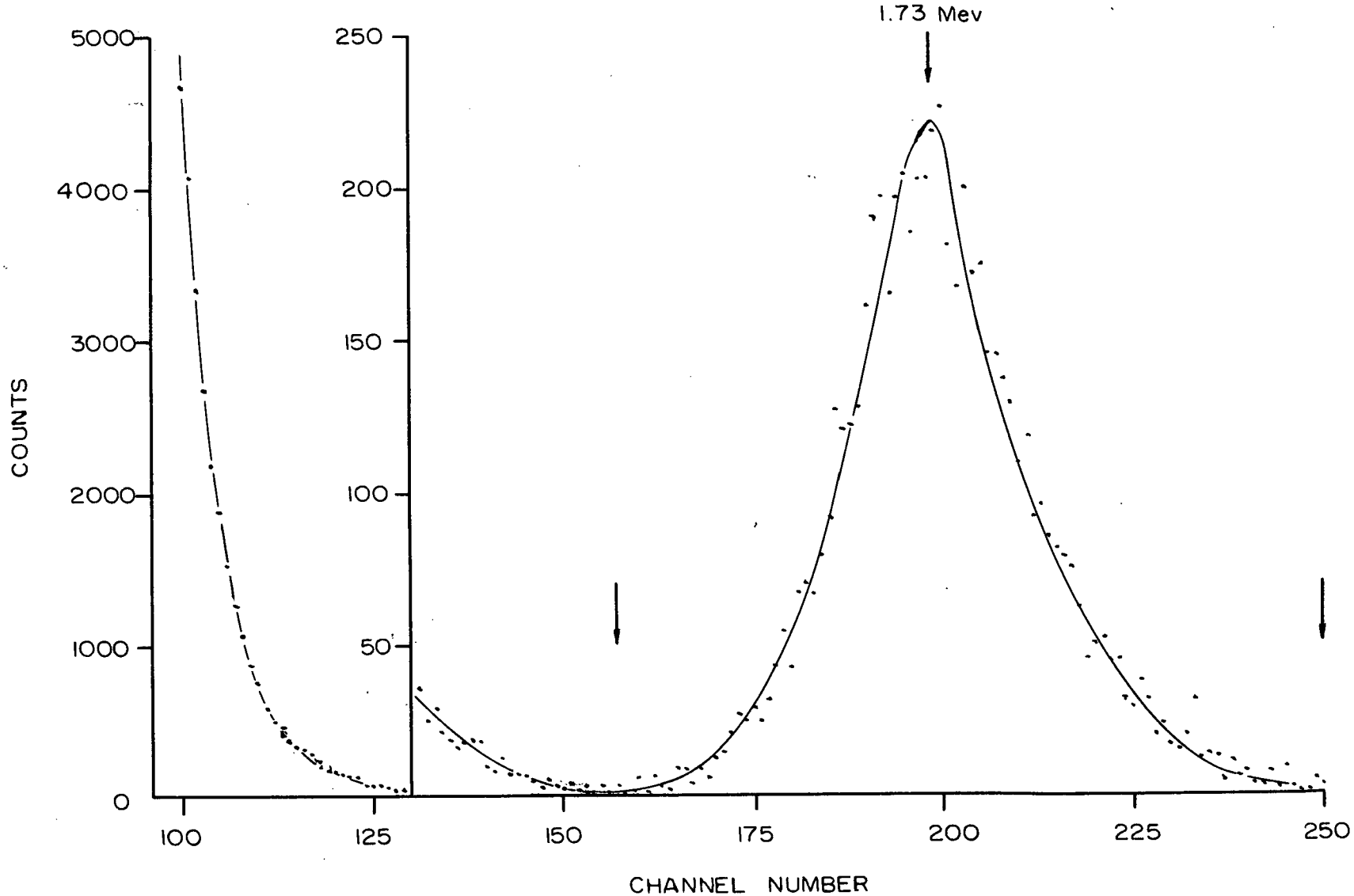

Fig. V-6 : Typical alpha spectrum from $^{19}F(p,\alpha\gamma)^{16}O$
The arrows show the region of summation.

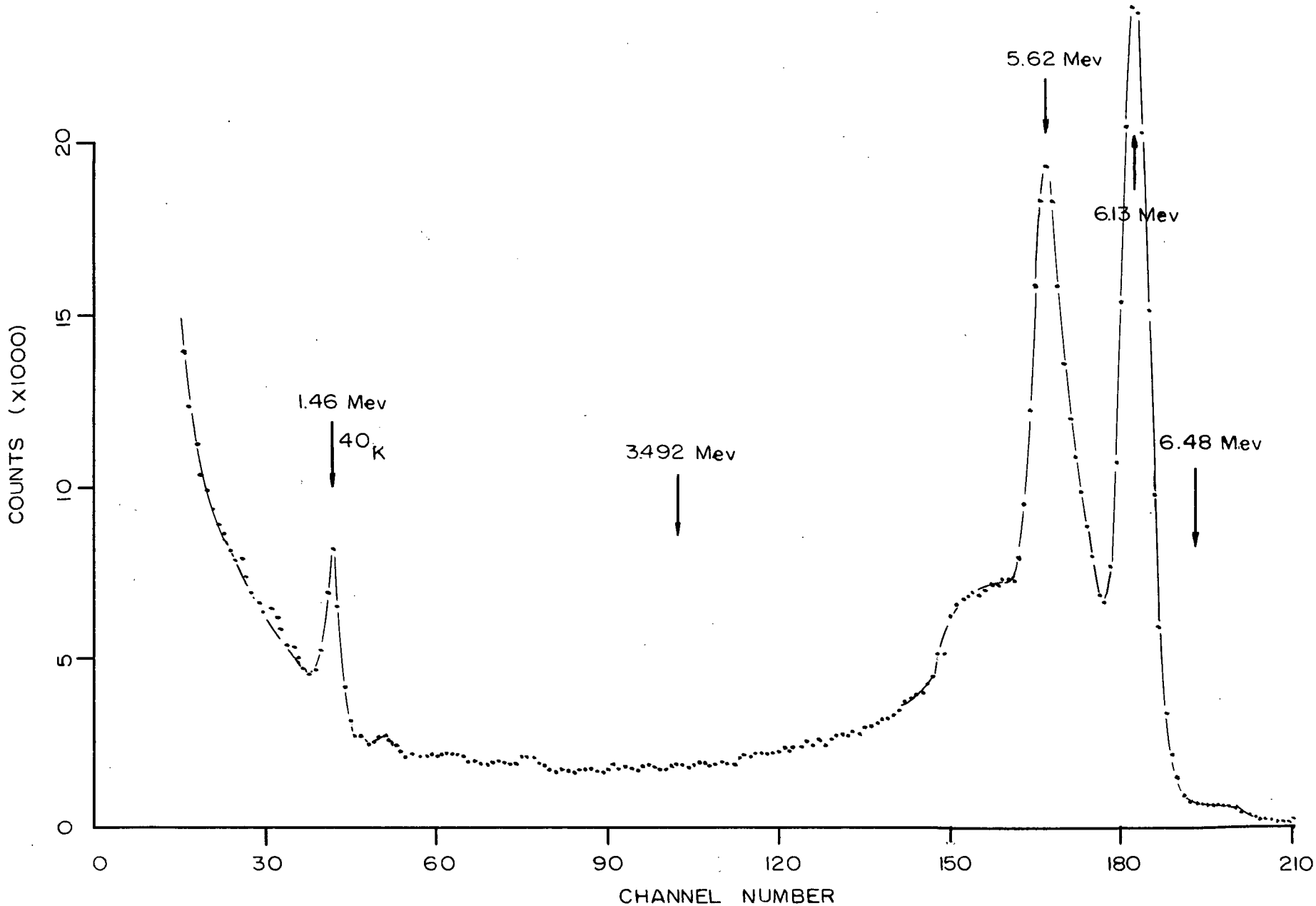

Fig. V-7 : Typical gamma spectrum from $^{19}F(p,\alpha\gamma)^{16}O$.

The errors quoted are standard deviations taken over several measurements.

(b) Gamma Detector

The main purpose for the measurement of the crystal efficiencies was so that the cross section for the reaction D $(p, \gamma)^3$He could be determined. It was decided that crystal D would be used for this purpose, fully collimated as shown in Figure III - 2. A summary of the dimensions applicable to the calculation of the solid angle has been given in Table III - 1.

An error occurred here, however, since an unreported change had been made to the collimator. Approximately 1.1 cm. had been shaved off the front end, and this was not known at the time that the measurements were made. Hence the gamma detector was actually set 1.1 cm. closer to the target than it should have been.

Since the cross section measurements were made at the proper distance, it was necessary to extrapolate the measured crystal efficiency to what it would have been at the proper distance by using a computed change of efficiency with distance. This correction was made by redefining the efficiency to be $A = \varepsilon\omega_\gamma$ where A is the absolute efficiency defined as the probability of a gamma ray emitted isotropically from the source being absorbed by the crystal.

The computer program DEWF which calculates the absolute efficiency of collimated gamma ray detectors, was used to obtain the theoretical absolute efficiency of the detector at the two source to crystal distances of interest. The correction was then applied in the following way. First the absolute efficiency was calculated using the data from the experimental runs. Then the expected experimental value for the proper source to crystal distance was predicted making use of the computer results referred to above. This was done

as a direct ratio between the experimental and computed absolute efficiencies at the two distances. Finally, the intrinsic efficiency for the proper distance was obtained by dividing the absolute efficiency by the solid angle subtended by the detector at the source. The solid angle is defined as shown in Figure III - 2.

In order to check that a large error was not being introduced by this method due to the efficiency not varying smoothly with distance, the theoretical absolute efficiency for several source to crystal distances was computed and plotted.

The results are shown in Figure V - 8. It is seen that the absolute efficiency follows an approximate inverse square behaviour as the distance between the source and crystal is varied. This is the familiar result for uncollimated detectors and it is of interest to note that the presence of the collimator does not cause a radical departure from this behaviour.

Arrow "A" shows the source to crystal distance used for the efficiency measurements; arrow "B" shows the proper source to crystal distance, taken from Table III - 1 (R = 19.52 cm.).

It was anticipated that the efficiency for crystal M might also be required at some time in the future, and also for both crystals uncollimated at the front face. These measurements were also taken.

For the purpose of getting the efficiency with the crystals uncollimated, the relevant geometry is shown in Figure V - 9, with the symbols and their dimensions listed in Table V - 3.

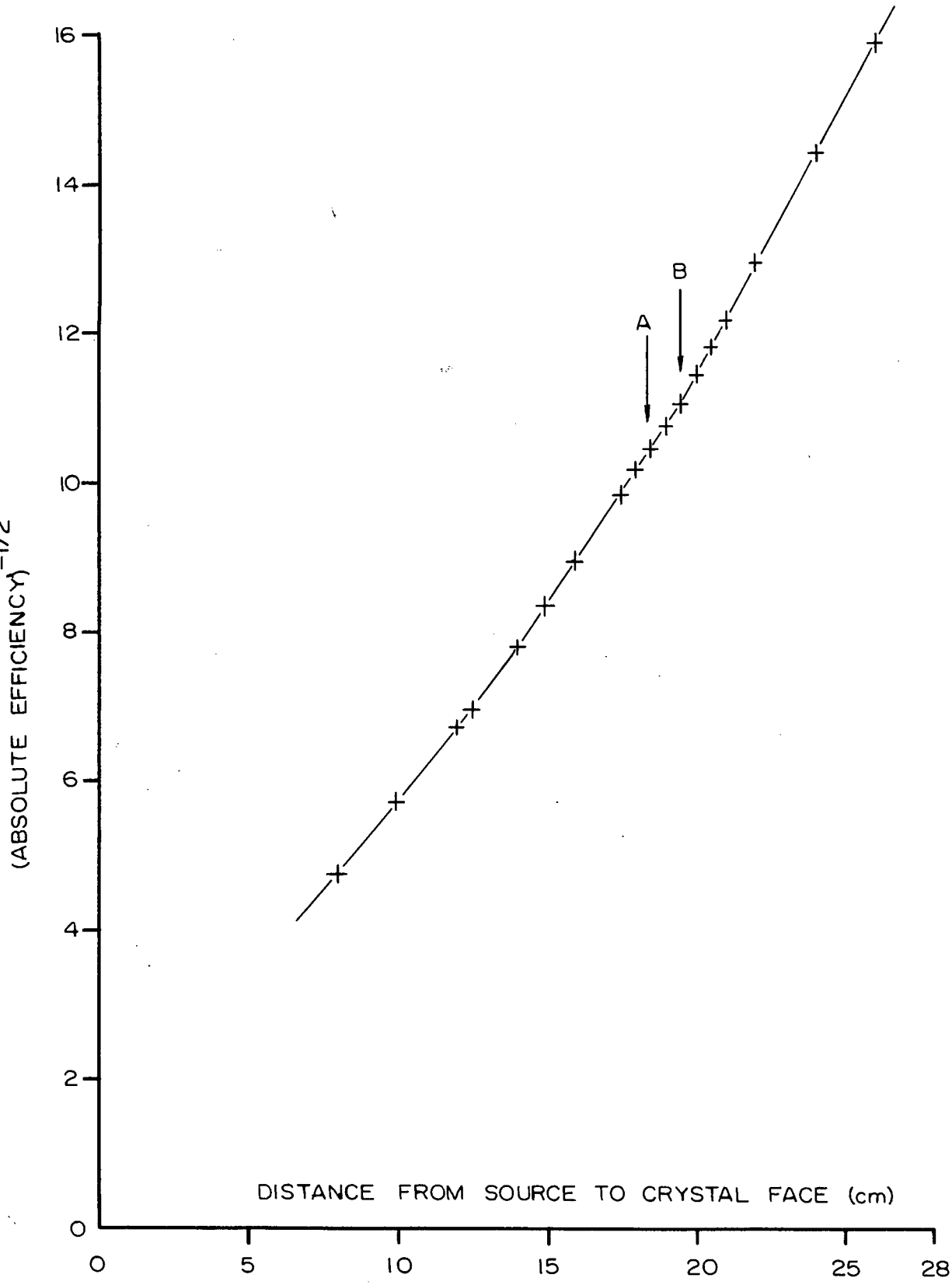

Fig. V-8 : Relation of absolute efficiency to distance.

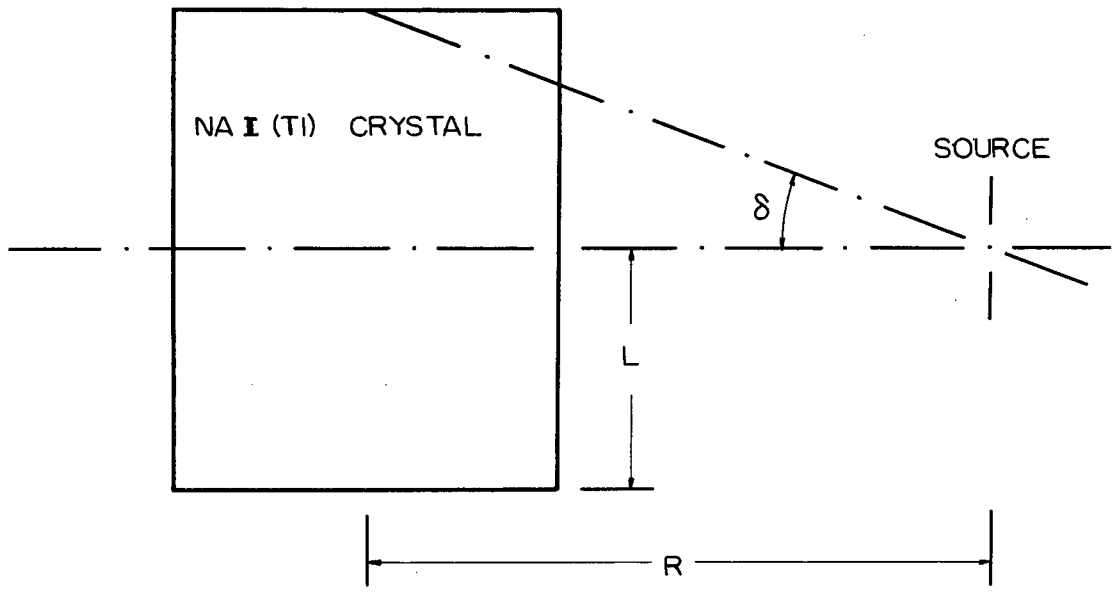

Fig. V-9 : Uncollimated gamma detector geometry.

Table V - 3: Uncollimated gamma detector geometry

Symbol	Distance
R	6.5 in.
L	2.5 in.
δ	21° 03'

The solid angle was taken from the source to the middle of the detector, and was calculated to be 0.571 steradians.

5-4. Results

After carefully checking the alignment of the target-detector system, an excitation function was again run on the target to locate the 340 kev resonance, and then all the efficiency runs were made at an energy 2 kev higher. The initial yield was approximately 4000 gamma counts per minute with from one-half to one microampere current on the target. The target was shifted whenever the number of gamma counts fell to 2000 counts per minute. It was necessary to run at the low beam current in order to maintain the dead time of the kicksorters below 2%. The time of the runs was determined by the time required to get approximately 6000 alpha counts, and was typically around three hours.

The number of alpha counts was summed from the minimum in the spectrum to the upper edge of the alpha counts (approximately channel 250), and was then corrected for dead time losses in the kicksorter. No correction was necessary for the α_2 and α_3 counts since the energy of these alphas after passing through the nickel window was considerably less than the lowest energy particles that were counted. The gamma counts were analyzed by the TREAT computer program, which gain-shifted all the results to the same settings as were used in the absolute cross-section analysis. This program then summed the counts from 3.492 Mev to 6.48 Mev -- the same limits as used for the

cross-section measurements -- and subtracted the appropriate amount of time dependent room background. These results were finally corrected for dead-time losses in the kicksorter and for absorption losses in the aluminum window and target backing. A small correction, based on the shape of the spectrum, was also applied to allow for the α_2 and α_3 gamma rays which were in the energy region of interest. No beam dependent background was subtracted since a run on a clean target backing showed that the correction would be less than 0.3 percent.

The absolute efficiencies were finally calculated as $A = \frac{N_\gamma}{N_\alpha} \omega_\gamma$ and the intrinsic efficiencies as $\varepsilon = A/\omega_\gamma$. The intrinsic efficiency for the proper collimated distance was determined in the way discussed previously. The intrinsic efficiency for the uncollimated crystals was calculated using the solid angle shown in Figure V - 9.

The results of the four measurements are listed in Table V - 4. The calculated error is less than 3 percent on all the measurements.

Table V - 4: Crystal efficiencies

Collimated crystals:-

	Absolute Efficiency		Intrinsic Efficiency	
Detector	Experiment	Proper Distance	Experiment	Proper Distance
D	.00838	.00743	.704	.679
M	.00864	.00769	.730	.702

Uncollimated crystals:-

Detector	Absolute Efficiency	Intrinsic Efficiency
D	.0218	.482
M	.0218	.482

CHAPTER VI

GAS TARGET AND ABSOLUTE CROSS SECTION

6.1 Introduction

The main sources of uncertainty associated with the measurement of an absolute cross section are the lack of precision in the knowledge of the number of nuclei in the target and the number of particles incident on the target. The latter is determined by integrating the charge collected by the target, and the former requires a knowledge of the target thickness.

It was originally hoped that the deuterated polyethylene target thickness could be found accurately by measuring the energy loss of alpha particles passing through it. These alphas were to originate from a source deposited onto the target backing before the polyethylene was poured on. However, drifts in the electronics made it impossible to measure accurately enough the location of the alpha peak (and hence the alpha energy) before and after putting on the polyethylene layer, so this method was discarded..

A second possibility for determining the target thickness was to measure the neutron yield from the $D(d,n)^3He$ reaction. However, this method was also discarded since it required knowing accurately the efficiency of the neutron counter, and it was expected that a large correction would be required for the beam dependent background for this efficiency measurement since the accelerator had just been used with a deuterium beam for some time.

Finally a decision was made to use a gas target, where the number of nuclei involved can be determined knowing the pressure of the gas and the length of the active volume. The following section describes the target used, and the method of determining the required parameters.

6.2 The Gas Target

One of the problems encountered in measuring the gas pressure involves local heating effects resulting from the passage of the incident beam through the gas. This heating causes the gas in the active volume to expand slightly, thus reducing the density in the region of the beam. To minimize the correction required for this effect the brass backstop of the target was made very large in the hope that the conduction would be great enough to maintain a constant temperature throughout the cell. The temperature of the backstop was monitored with a copper-constantin thermocouple which was inserted into a hole drilled into the stop. No appreciable difference could be detected between the stop temperature and room temperature with the beam on the target.

A first attempt to measure the effect of local heating by passing beams through the gas cell with varying currents had also failed because of a slow carbon buildup on the foil while the runs were taking place. This carbon buildup produced an energy loss in the incident beam with an error larger than the effect being studied. However, the effect has been measured previously in this way (RO 61) using deuterium gas but at a higher pressure. After making the appropriate allowances for the different pressure, it was found that, with the beam current used for the cross section measurements, the gas in the beam path was 0.8% less dense than that in the remainder of the target chamber, the pressure of which was measured with a manometer.

The entrance window to the gas target was a 30 micro-inch nickel foil obtained from the Chromium Corporation of America. This foil thickness was chosen as a compromise among the following factors: the strength required to withstand the gas pressure, a minimum energy loss and straggling of the beam in passing through the foil, and a maximum allowable beam current. The energy loss was measured by noting the shift of the 992 kev resonance of the $^{27}Al\ (p, \gamma)^{28}Si$ reaction with the foil in place, and then correcting for the

stopping cross section difference between this energy and 780 kev and 800 kev, the energies at which the absolute cross section were measured. The foil thickness was found in this way to be 127 kev at 780 kev incident proton energy.

The maximum allowable beam current for 780 kev incident protons is approximately 0.8 microampere according to curves published in the 1960 Nuclear Data Tables (Part 3, P. 124); the runs were made at a current of 0.5 microamperes.

The length of the gas cell was determined by first measuring with a travelling microscope the distance between the foil holder and the backstop. Now the gas in the cell causes the foil to depress slightly, and this depression was measured by noting the different focussing locations of the travelling microscope when focussed on the edge of the holder compared to when it was focussed on the point where the beam passed through the foil. The length was determined to be $1.019 \pm .002$ cm.

The average energy of the proton beam in the gas cell can be determined by subtracting from the incident beam energy the energy loss as the beam passes through the foil, and one-half the energy loss of the beam as it passes through the gas. This latter quantity was determined by the computer program ENLOTA, which subdivides the gas cell length into several elements of length, and then computes the energy loss in each small sub-length. In this way, the variation in the stopping cross section of the gas with energy is allowed for. For 800 kev and 780 kev incident proton energies, the average energy in the gas cell was found to be 663 kev and 643 kev respectively.

The gas pressure was measured with a U-tube manometer filled with mercury. Provision was made to evacuate both arms of the tube and then, by closing a glass tap, one of these could be isolated from the main system prior to filling the gas cell. This enabled the pressure in the cell to be read directly as the difference in the level of mercury in the two arms. After filling the cell, a

glass tap on the other arm was also closed to prevent any mercury contamination in the system.

Other features of the target include an all-brass construction except for a lucite window on one side through which the beam could be viewed hitting the backstop, and an aluminum window on the other side through which the gamma rays passed on their way to the detector.

The collimators were made of platinum with a view to reducing the contaminant background radiation, especially that arising from $^{19}F(p,\alpha\gamma)^{16}O$, since previous tests had indicated that platinum had the least contaminating material. For this same purpose, a piece of platinum was attached to the face of the backstop where the beam hit it.

A diagram of the target with the nickel foil holder, collimators and electron suppression assembly and gas filling device is shown in Figure VI - 1.

6.3 Current Integration

The other problem associated with measuring the cross section was an accurate determination of the charge delivered to the gas target by the beam. The first point of concern here is the ejection of secondary electrons from the backstop, which would result in an effective increase in the positive charge measured. To overcome this difficulty, a positive bias was put on the backstop to prevent the electrons from escaping. This introduces a second problem, however, which results from the ionization of the gas as the beam passes through it. If the backstop is positively biased and the rest of the target assembly, including the nickel foil, is unbiased, then the negative ions will drift to the backstop and the positive ions to the foil and chamber walls. This will result in a decrease in the amount of positive charge measured. Hence the foil, target chamber and backstop must all be at the same potential. In this experiment, +90 volts was used.

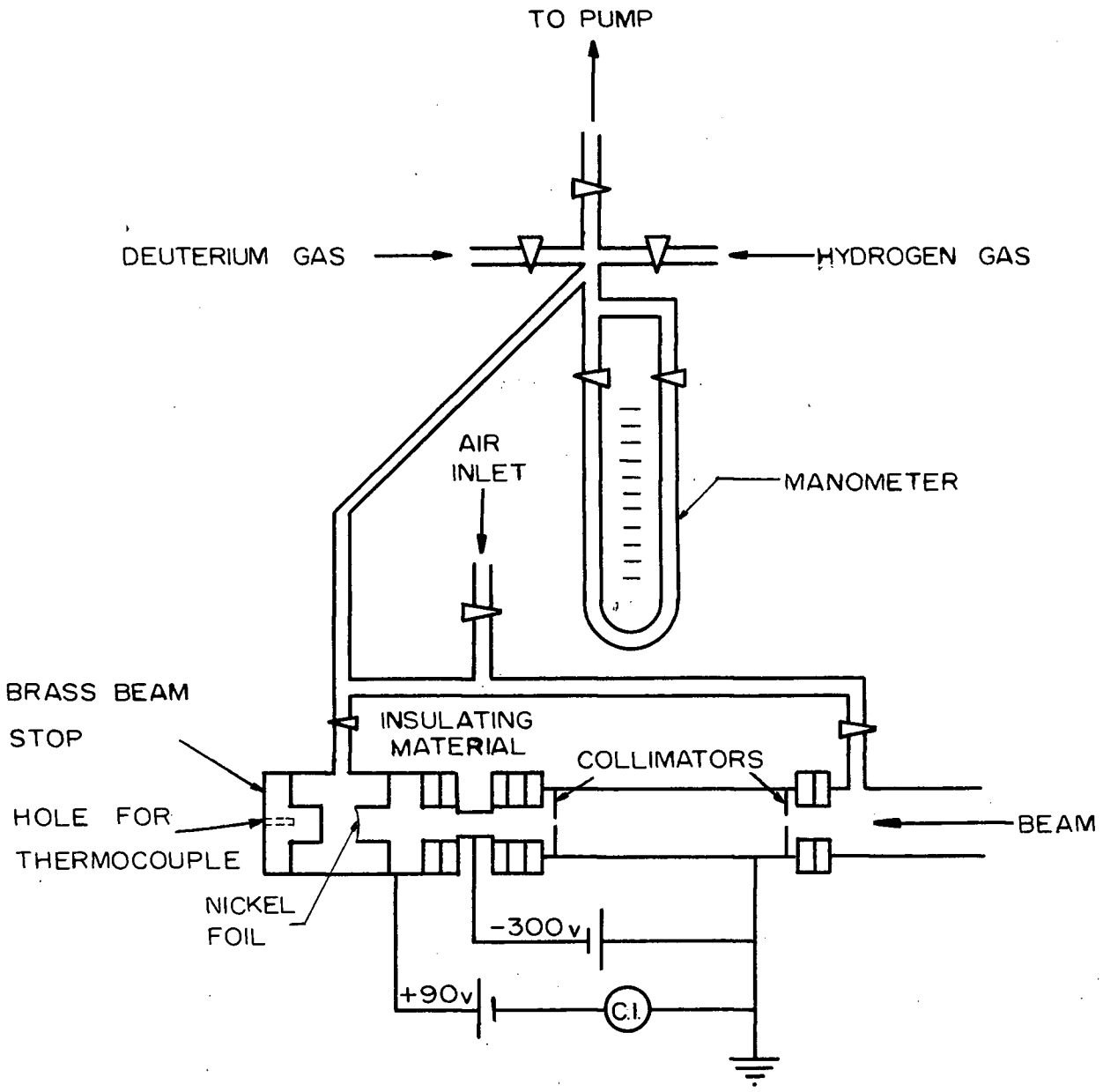

Fig. VI-1 : The gas target assembly.

The positive bias on the nickel foil has the added benefit that copious numbers of electrons, which would otherwise be ejected from the foil, are prevented from escaping. A problem did arise from the fact that the foil and the foil holder were tied to the backstop. It was necessary that no protons hit the edges or sides of the holder; otherwise charge is collected which has not passed through the gas. To prevent this from happening, a collimator system was designed to limit the diameter of the beam to less than 0.1 inch, whereas the width of the foil which was exposed to the incident beam was 0.3 inch. A check was made to ensure that the beam was not diverging by inserting a quartz backstop into the target chamber. An end-on view of the proton beam was thus available.

Finally, any secondary electrons which might be emitted from the edges of the collimators must be prevented from reaching the foil assembly. To this end, a suppressor with a -300 volt bias was placed in the beam line between the collimators and the foil holder.

The current measured in the target chamber was fed to an Eldorado Electronics Current Integrator, Model CI - 110, the same as used during the relative cross section measurements. Very careful calibration of the current integrator was of course required since any error arising here would be transmitted directly to the cross-section.

The calibration was carried out using a Weston Standard Cell and a Gambrell precision resistor. The accuracy of the standard cell was checked using two different resistance bridges (Electro Scientific Industries Model 250DE Impedance Bridge and Model 300 Potentiometric Voltmeter-Bridge). The difference between the measured value and the quoted value for both the cell and the resistor was found to be less than the error of the measuring instruments. The error of the combination of standard cell and precision resistor was taken to be less than two parts in a thousand.

The method of calibrating the current integrator was to feed in a current on the current range used during the cross-section runs, and then to compare the charge integrated for this known current and known time to the charge which was expected. A summary of the results of this calibration is shown in Table VI - 1.

Table VI - 1. Current integrator calibration

Known Current	1.0185 $\pm$ .001 uamps
Known Time	1138.5 $\pm$ 3.5 sec.
Known Charge (Known Current x Known Time)	1159.6 $\pm$ 3.5 ucoul
Charge Setting on the Current Integrator	1200 ucoul

This table shows that the actual integrated charge is 96.6 $\pm$ 0.4 percent of the charge indicated by the current integrator and this correction was applied to the final results.

6.4 Experimental Procedure

The collimated NaI (Tl) detector (D crystal) was placed at 90° to the incident beam in order to obtain the maximum yield of gamma rays from the reaction. The cross hairs on the collimator, previously described in the section on the crystal efficiency, were used to ensure that the detector was aiming at the centre of the target. The crystal was set at the proper collimated distance from the centre of the target by measuring the distance from the front face of the crystal to a mark in the centre of the outside face of the backstop.

The data collection from the detector was accomplished using the same electronic arrangement used for the measurement of the crystal efficiencies, except that the ND 160 was used in place of the ND 120. A scaler was again employed so that the number of counts obtained in a given time interval could

be periodically monitored to ensure that all the equipment was performing satisfactorily.

Finally, the measurement of the cross section was broken down into five separate runs in order to reduce the risk of losing all the data if something were to go wrong, such as the foil breaking or large drifts occurring in the electronics, and to average out any small background variations. Each run took approximately 4 hours and was further split up into two parts, one with deuterium in the gas cell, and the other with hydrogen. In this way the beam dependent background could be accounted for by subtracting the hydrogen run directly from the deuterium. This method proved practical since no large buildup of background occurred during any one particular run. A correction was also applied for the time dependent background, but this was very small since it was necessary to take into account only the time difference between a hydrogen run and a deuterium run. The deuterium was obtained from the Liquid Carbonic Division of General Dynamics, and had a quoted purity of 99.7 percent.

In order to change the gas in the cell, the cell was first evacuated, then flushed with the new gas and evacuated again before the final filling took place. The runs were made with approximately 150 mm Hg gas pressure in the cell, measured with the manometer previously described.

The total integrated charge was 2400 microcoulombs per run for four of the runs and 3600 microcoulombs for the other. A correction was then applied to the charge collected to allow for the error in the current integrator, which has been described previously.

6.5 Other Corrections Factors

Reference to equation (2.1 -5) and the ensuing discussion shows that the solid angle subtended by the detector and the angular distribution factor

$[1 + \frac{A_2}{A_0} P_2 Q_2 + \frac{A_1}{A_0}(P_1 Q_1 - P_3 Q_3)]$ must also be determined in order to compute the cross section. A small correction must also be applied to the detector efficiency, since this was measured with 6.14 Mev gamma rays compared to the 5.92 Mev gamma rays obtained from the reaction $D(p, \gamma)^3He$ at a proton bombarding energy of 643 kev, which was the average proton energy in the gas cell.

The solid angle was calculated from the data listed in Table III - 1. for Figure III - 2. and was found to be 0.1376 $\pm$ .0006 steradians.

To determine the angular distribution factor, use is made of the data listed in Tables II - 1. and II - 2. The Legendre polynomials were calculated for centre of mass angles, and it is found that an angle of 90° in the laboratory frame corresponds to 90.71 degrees in the centre of mass frame. Thus the angular distribution factor was calculated to be 1.4624.

In order to determine the efficiency change of the detector, use was made of the computer programs LFIT and SHAPE. These programs used in conjunction with each other produce from known gamma ray shapes at various energies interpolated gamma ray shapes for intermediate energies. Thus the standard shape for the 5.92 Mev gamma rays from the $D(p, \gamma)^3He$ reaction was found.

Consider two gamma rays, the 5.92 Mev $D(p,\gamma)^3He$ radiation and the 6.14 Mev $^{19}F(p,\alpha\gamma)^{16}O$ radiation for which the absolute efficiency has been determined. Now if each standard gamma ray spectrum has the same number of counts in the total spectrum and is plotted for the same energy gain and zero, and we assume that the two gamma rays have approximately the same energy so that the shapes of the two spectra can be considered to be the same, then the ratio between the number of counts in a given energy region of the two spectra will give the relative efficiency of the detector for the two gamma rays, provided that the upper limit of the energy region considered is above the full photopeak, and the lower limit is approximately one-half the full energy, or lower.

It was found that over the chosen energy region from 3.492 Mev to

6.48 Mev, there were 991.4 counts of the 5.92 Mev radiation and 1000 counts of the 6.14 Mev radiation. Hence the efficiency for the D detector which was found as described in the last chapter was multiplied by .9914 to allow for the change in energy of the gamma ray.

Two other corrections, both of which resulted in a modification to the number of detected gamma rays, were required. The first of these arose from dead time losses in the kicksorter, and resulted in a factor of 1.003 increase in the number of gamma rays detected. The second arose from absorption losses through the aluminum window, and required a factor of 1.006 increase.

Finally, the pressure in the gas cell was corrected for the density change of mercury with temperature, since the measurements were not made at the standard temperature and pressure.

6.6 Results

The spectra, which were obtained from the five runs--each consisting of one hydrogen and one deuterium part--were gain-shifted to the same gain and zero by the computer program TREAT, and then were summed over the energy region 3.492 Mev to 6.48 Mev. The appropriate corrections which have just been described were then applied to these results, and the absolute cross section was calculated for each run. The results of these calculations are listed in Table VI - 2. The error quoted with each result is the root mean square error of the quantities which contribute to the cross section.

Table VI - 2: Absolute cross section measurement

Laboratory Proton Energy	Absolute Cross Section
663 kev	$2.33 \pm .10$ microbarns
663 kev	$2.57 \pm .11$
643 kev	$2.35 \pm .10$
643 kev	$2.28 \pm .10$
643 kev	$2.42 \pm .11$

The measurements made at 663 kev were converted to the equivalent 643 kev result making use of an approximate expression for the cross section given in the paper by Fowler et al which has been discussed previously. This expression is

$$= KE^{n} \times 10^{-29} cm^{2} \qquad (6.6 - 1)$$

where $K = 0.74 \pm 50\%$

$n = 0.72 \pm 15\%$

and E is the laboratory energy in Mev.

It is found that this conversion gives the first run a result of 2.28 microbarns and the second a result of 2.51 microbarns.

The result of the second run seems inconsistent with the other four, and hence was discarded. No reason for the discrepancy was readily apparent.

The result of averaging the other four runs gives the cross section as $2.33 \pm .07$ microbarns, where the error is the standard deviation of the four runs. Thus the absolute cross section is effectively determined for the entire range of values over which the relative cross section was measured. Figure VI-2 shows these results, and the results of previous measurements made in this laboratory.

The present work gives quite good agreement with the previous results,

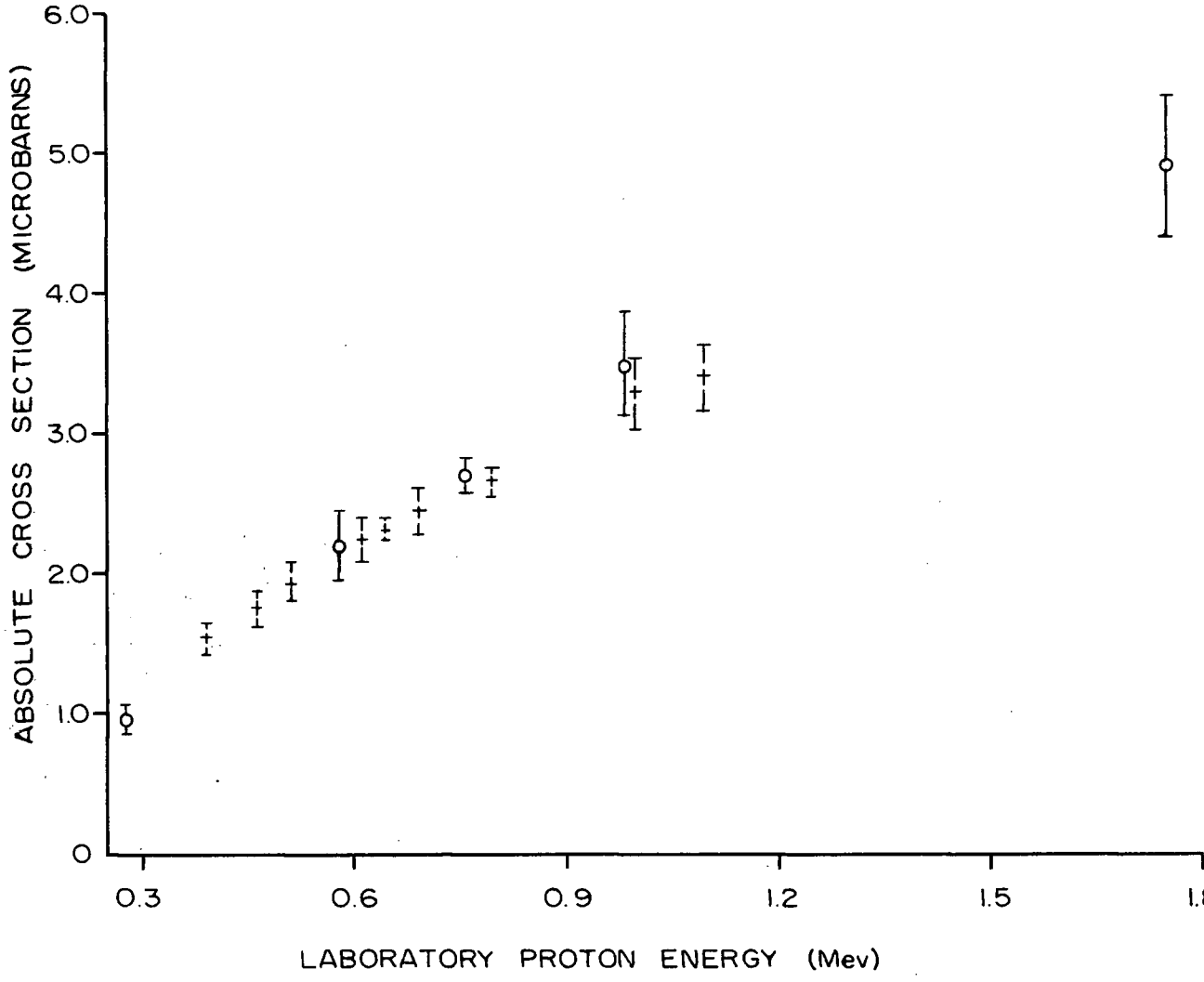

Fig. VI-2 : The absolute cross section for the reaction $D(p,\gamma)^3He$. The circles are the results of Griffiths et. al. (GR 61). The crosses are the present measurements.

although at higher energies the present results seem to be slightly lower. This is possibly due to an incomplete subtraction of the fluorine contamination in the earlier measurements.

BIBLIOGRAPHY

BA 69 G.M.Bailey, to be published.

CH 50 C.Y.Chao, A.V.Tollestrup, W.A.Fowler and C.C.Lauritsen, Phys. Rev., 79 (1950) 108

DE 49 S.Devons and M.G.N.Hine, Proc. Roy. Soc. (London) 199A (1949) 56.

DE 60 G.Derrick, Nucl. Phys. 16 (1960) 405.

DO 67 T.W.Donnely, Ph.D. Thesis, University of British Columbia (1967).

FO 49 W.A.Fowler, C.C.Lauritsen and A.V.Tollestrup, Phys. Rev., 76 (1949) 1767.

FR 50 J.M.Freeman, Phil. Mag. 41 (1950) 1225.

GR 55 G.M.Griffiths and J.B.Warren, Proc. Phys. Soc., 68 (1955) 781.

GR 61 G.M.Griffiths, E.A.Larson, and L.P.Robertson, Can. J. Phys. 40 (1962) 402.

GR 63 G.M.Griffiths, M.Lal and C.D.Scarfe, Can. J. Phys., 41 (1963) 724.

LA 57 E.A.S. Larson, M.A. Thesis, University of British Columbia (1964).

LE 64 J.L. Leigh, M.Sc. Thesis, University of British Columbia (1964).

OL 68 M.A. Olivo, Ph. D. Thesis, University of British Columbia (1968).

RO 53 M.E. Rose, Phys. Rev., 91 (1953) 610.

RO 61 L.P. Robertson, B.L.White and K.L. Erdman, Rev. Sci. Inst., 32 (1961) 1405.

VE 50 M. Verde, Helv. Phys., Acta 23 (1950) 453.

WI 52 D.H. Wilkinson, Phil. Mag., 43 (1952) 659.

WO 67 W.Wolfli, R. Bosch, J.Lang, R. Muller, and P. Marmier, Helv. Phys. Acta, 40 (1967) 946.

APPENDIX

COMPUTER PROGRAMS

DEWF : This program calculates the absolute detection efficiency of scintillation crystals for gamma rays, and the weighting (Q) factors that compensate for the finite solid angle of the counter.

LFIT : The input to this program is a number of standard gamma ray shapes of various energies. The full peak of each input spectrum appears in the same channel and has the same number of counts as all the other spectra, and all spectra have the same gain. The program then does a cubic fit of the counts versus energy relation for each channel of the input spectra. The output is a matrix giving the four coefficients from the cubic fit for each channel.

SHAPE : The input to this program is the output from LFIT. The program then determines the number of counts in each channel for a gamma ray of a specified energy. Thus LFIT and SHAPE used in conjunction interpolate the shape of a specified gamma ray from several given gamma rays.

TREAT ; This is a general purpose program for the preliminary treatment of data prior to the detailed analysis done by NAILS. The program can be used to smooth the data, gain-shift it, and sum the counts between two given energies. Up to eight spectra can be subtracted from or added to the spectrum being treated.

NAILS : This program is used to determine by an iterative least squares procedure the relative amounts of various specified components in a given spectrum. Included in the output is an estimate of the accuracy of the results based on the differences of the intermediate iterations with

the final results. The input to NAILS was usually the output of TREAT.

POLY-D : This program corrects for the deterioration of deuterated polyethylene targets by fitting the target decay with the sum of two exponentials.

CSFIT : This program fits both of the relative cross section results of the two detectors with a cubic least squares curve, and then multiplies one of these curves by a constant factor to give the best fit with the other.

ENLOTA : This program calculates the energy loss of a beam when passing through a gas target. Allowance is made for the variation of the stopping power of the gas with energy.